



A novel triazole, NMK-T-057, induces autophagic cell death in breast cancer cells by inhibiting γ -secretase-mediated activation of Notch signaling

Received for publication, January 25, 2019. Published, Papers in Press, March 1, 2019, DOI 10.1074/jbc.RA119.007671

Amlan Das,^{a,b1,2} Maruthi Kumar Narayanam,^{c,d3} Santanu Paul,^{a1,3} Pritha Mukherjee,^{e3} Suvranil Ghosh,^f Debabrata Ghosh Dastidar,^{a,g} Subhendu Chakrabarty,^a Arnab Ganguli,^a Biswarup Basu,^h Mahadeb Pal,^f Urmi Chatterji,^e Sushanta K. Banerjee,^{ij} Parimal Karmakar,^k Dalip Kumar,^{c4} and Gopal Chakrabarti^{a5}

From the ^aDepartment of Biotechnology and Dr. B. C. Guha Centre for Genetic Engineering and Biotechnology and ^eDepartment of Zoology, University of Calcutta, 35 Ballygunge Circular Road, Kolkata 700019, West Bengal, India, ^bDepartment of Chemistry, National Institute of Technology, Ravangla, South Sikkim 737139, India, ^cDepartment of Chemistry, Birla Institute of Technology and Science, Pilani, Rajasthan 333031, India, ^dDivision of Molecular Medicine, Bose Institute, P-1/12, CIT Road, Scheme VIIM, Kankurgachi, Kolkata 700054, West Bengal, India, ^fDivision of Pharmaceutical Sciences, Guru Nanak Institute of Pharmaceutical Science and Technology, 157/F Nilgunj Road, Panihati, Kolkata 700114, West Bengal, India, ^gDepartment of Experimental Hematology and Neuroendocrinology, Chittaranjan National Cancer Institute, 37 Shyama Prasad Mukherjee Road, Kolkata 700026, West Bengal, India, ^hCancer Research Unit, Veterans Affairs Medical Center, Kansas City, Missouri 64128, ⁱDepartments of Anatomy and Cell Biology and Pathology, University of Kansas Medical Center, Kansas City, Kansas 66160, ^jDepartment of Molecular and Medical Pharmacology and Crump Institute for Molecular Imaging, David Geffen School of Medicine, UCLA, Los Angeles, California 90095, and ^kDepartment of Life Science and Biotechnology, Jadavpur University, 188 Raja S. C. Mullick Road, Kolkata 700032, Western Bengal, India

Edited by George N. DeMartino

Notch signaling is reported to be deregulated in several malignancies, including breast, and the enzyme γ -secretase plays an important role in the activation and nuclear translocation of Notch intracellular domain (NICD). Hence, pharmacological inhibition of γ -secretase might lead to the subsequent inhibition of Notch signaling in cancer cells. In search of novel γ -secretase inhibitors (GSIs), we screened a series of triazole-based compounds for their potential to bind γ -secretase and observed that 3-(3',4',5'-trimethoxyphenyl)-5-(*N*-methyl-3'-indolyl)-1,2,4-triazole compound (also known as NMK-T-057) can bind to γ -secretase complex. Very interestingly, NMK-T-057 was found to inhibit proliferation, colony-forming ability, and motility in various breast cancer (BC) cells such as MDA-MB-231, MDA-MB-468, 4T1 (triple-negative cells), and MCF-7

(estrogen receptor (ER)/progesterone receptor (PR)-positive cell line) with negligible cytotoxicity against noncancerous cells (MCF-10A and peripheral blood mononuclear cells). Furthermore, significant induction of apoptosis and inhibition of epithelial-to-mesenchymal transition (EMT) and stemness were also observed in NMK-T-057-treated BC cells. The *in silico* study revealing the affinity of NMK-T-057 toward γ -secretase was further validated by a fluorescence-based γ -secretase activity assay, which confirmed inhibition of γ -secretase activity in NMK-T-057-treated BC cells. Interestingly, it was observed that NMK-T-057 induced significant autophagic responses in BC cells, which led to apoptosis. Moreover, NMK-T-057 was found to inhibit tumor progression in a 4T1-BALB/c mouse model. Hence, it may be concluded that NMK-T-057 could be a potential drug candidate against BC that can trigger autophagy-mediated cell death by inhibiting γ -secretase-mediated activation of Notch signaling.

This work was partially supported by a University with Potential for Excellence (UPE)-II grant from the Government of India (to G. C.). The authors declare that they have no conflicts of interest with the contents of this article.

This article contains Figs. S1–S5 and Tables S1 and S2.

¹ Supported by Dr. D. S. Kothari Postdoctoral Fellowship (DSKPDF) BL/15-16/0193 and Fellowship F.42/2006 (BSR)/BL/1617/0351 from the University Grants Commission, Government of India.

² To whom correspondence may be addressed: Dept. of Biotechnology and Dr. B. C. Guha Centre for Genetic Engineering and Biotechnology, University of Calcutta, 35 Ballygunge Circular Rd., Kolkata 700019, West Bengal, India. Tel.: 91-33-2461-5445; Fax: 91-33-2461-484. Dept. of Chemistry, National Institute of Technology, Ravangla, South Sikkim 737139, India. Tel.: 91-8670364931; Fax: 91-03595-260042; E-mail: adas1980@nitsikkim.ac.in.

³ These authors contributed equally to this work.

⁴ To whom correspondence may be addressed: Dept. of Chemistry, Birla Institute of Technology and Science, Pilani 333031, Rajasthan, India. Tel.: 91-1596-24507; Fax: 91-1596-244183; E-mail: dalipk@pilani.bits-pilani.ac.in.

⁵ To whom correspondence may be addressed: Dept. of Biotechnology and Dr. B. C. Guha Centre for Genetic Engineering and Biotechnology, University of Calcutta, 35 Ballygunge Circular Rd., Kolkata 700019, West Bengal, India. Tel.: 91-33-2461-5445; Fax: 91-33-2461-4849; E-mail: gcbcg@caluniv.ac.in.

Breast cancer (BC)⁶ is the most common cancer in women and accounts for almost 15% of all cancer-related deaths in

⁶ The abbreviations used are: BC, breast cancer; NICD, Notch intracellular domain; GSI, γ -secretase inhibitor; NMK-T-057, 3-(3',4',5'-trimethoxyphenyl)-5-(*N*-methyl-3'-indolyl)-1,2,4-triazole compound; ER, estrogen receptor; PR, progesterone receptor; PBMC, peripheral blood mononuclear cell; TNBC, triple-negative breast cancer; PSEN-1, Presenilin-1; APH-1, anterior pharynx-defective 1; PTEN, phosphatase and tensin homolog; NMK, NMK-T-057; PI, propidium iodide; BW, body weight; SGOT, serum glutamate oxaloacetate transaminase; SGPT, serum glutamate pyruvate transaminase; ALP, alkaline phosphatase; EMT, epithelial-to-mesenchymal transition; ALDH, aldehyde dehydrogenase; CSC, cancer stem cell; TIC, tumor-initiating cell; pAkt, phosphorylated Akt; DAPT, *N*-[*N*-(3,5-difluorophenacetyl)-*L*-alanyl]-*S*-phenylglycine *t*-butyl ester; dnp, 2,4-dinitrophenyl; NMA, *N*-methyl aspartic acid; LC3, light chain 3; MDC, monodansylcadaverine;

NMK-T-057 inhibits γ -secretase-mediated Notch activation

women worldwide (1, 2). In recent years, the rate and incidence of BC have increased in India at an alarming rate. Presently, BC is the most common cancer in the female population, preceding cervical cancer, in India with a very high mortality rate (3, 4). BC may be classified into distinct molecular subtypes, including normal-like, luminal A and B, HER2⁺, and basal-like (5). The basal-like subtype, also known as triple-negative breast cancer (TNBC) due to the absence of estrogen receptor (ER), progesterone receptor (PR), and HER2, is characterized by resistance to chemotherapy, acquisition of stemness, and poor prognosis (6, 7). Hence, development of novel drug candidates against BCs as well as identification of novel cellular targets has become a major thrust area of research.

The Notch signaling pathway has been reported to be highly deregulated in several human malignancies, including lung, cervical, colon, pancreatic, and renal carcinoma to name a few (8–11). It has also been reported that elevated expression levels of Notch-1 and its ligand Jagged-1 are associated with the poor prognosis, lower survival rate, and development of chemoresistance in breast cancer (12–17). Moreover, Notch signaling is also known to be the key regulator of stemness in breast cancer (18–20). Hence, targeting Notch signaling has gained immense importance in the development of novel anticancer regimes against breast cancer (19, 21, 22).

Activation of Notch signaling requires the interaction between Notch receptor and its ligand Jagged-1 or Jagged-2 followed by a series of proteolytic cleavages. Notch receptors are transmembrane heterodimeric proteins consisting of an extracellular domain, a transmembrane domain, and a cytoplasmic domain (17). The initial cleavage, or S1, of the Notch precursor is initiated in the Golgi network by a furin-like convertase to generate a heterodimeric receptor at the cell surface (23). Binding of Notch receptor to its ligands triggers the second, or S2, cleavage. This is catalyzed by a family of metalloendopeptidases known as ADAM (a disintegrin and metalloproteinase) or TACE (tumor necrosis factor- α -converting enzyme), which cleaves the Notch receptor at an extracellular site (S2) between Ala (1710) and Val (1711) residues, thus releasing a fragment, known as Notch extracellular domain (24). The remaining receptor fragment then undergoes the third proteolytic cleavage (S3) by a membrane-bound protease known as γ -secretase complex to release the activated Notch intracellular domain (NICD) into the cytosol (24). γ -Secretase is a multisubunit enzyme complex consisting of four subunits, namely Presenilin-1 (PSEN-1), Nicastrin, anterior pharynx-defective 1 (APH-1), and Presenilin enhancer 2 (PEN-2). Presenilin is an aspartyl protease that forms the catalytic core, whereas Nicastrin is required for substrate recognition (24). The activated NICD then translocates to the nucleus and modulates the transcription of its downstream targets genes such as Hes-1, Hey-1, Akt, and PTEN (21, 25). Due to its important role in the activation of Notch signaling, γ -secretase complex has become

a potential target for specific inhibitors, known as γ -secretase inhibitor (GSIs), which are reported to show significant anticancer properties against several carcinomas, including breast, and a few of them have also entered phase I and phase II clinical trials (26, 27).

In search of novel GSIs, we investigated the Notch inhibitory properties of a triazole-based compound, 3-(3',4',5'-trimethoxyphenyl)-5-(N-methyl-3'-indolyl)-1,2,4-triazole (also known as NMK-T-057), consisting of 1,2,4-triazole ring linked with an indole moiety (Fig. 1A). The presence of an indole ring system is known to attribute diverse medicinal and pharmacological properties to small molecules of both natural and synthetic origins (28). When the indole ring is linked with five-member heterocyclic triazoles, the resultant compounds have been reported to gain potent anticancer properties (29). Moreover, available literature indicates that 1,2,4-triazole derivatives possess potent anticancer properties (29–31) and are also effective against breast cancer cells (32, 33). Hence, in the present study, we have investigated the anticancer mechanism of the novel indolyl triazole derivative NMK-T-057 against several breast cancer cell lines by monitoring different oncogenic parameters, including migratory properties, epithelial-to-mesenchymal transition, and stemness. Because Notch signaling is known to be a regulator of epithelial-to-mesenchymal transition (EMT) and stemness in BC (34, 35), we also investigated whether NMK-T-057 can target Notch signaling in BC cells. To delineate the specific mechanism of Notch inhibition by NMK-T-057, we monitored γ -secretase activity in NMK-treated cells. Furthermore, it has been reported that inhibition of Notch signaling leads to autophagic cell death in BC cells (36, 37). Hence, we have also investigated whether inhibition of γ -secretase-mediated Notch activation by NMK-T-057 leads to autophagic cell death in BCs. Thus, the present study highlighted a very specific mechanism by which the triazole-based drugs can inhibit BC cells.

Results

NMK-T-057 inhibits the oncogenic potential of BC cells with minimal toxicity in Swiss albino mice

Treatment of TNBC cells such as MDA-MB-231, MDA-MB-468, and 4T1 and non-TNBC cell type MCF-7 with NMK-T-057 for 24 h resulted in the loss of viability in a dose-dependent manner (Fig. 1, B and C). However, comparatively lesser cytotoxicity was observed when noncancerous cell types such as MCF-10A and peripheral blood mononuclear cells (PBMCs) were treated with NMK-T-057, with respective IC₅₀ values >50 μ M. Effects of NMK-T-057 on TNBCs such as MDA-MB-231, MDA-MB-468, and 4T1 cells were more or less similar, with the observed IC₅₀ values ranging between 8 and 12 μ M, whereas MCF-7 was found to be most susceptible to NMK-T-057, with the IC₅₀ observed at 5 μ M (Fig. 1C).

The colony-forming ability of BC cells such as MDA-MB-231 and MCF-7 cells in the presence or absence of NMK-T-057 was determined by *in vitro* clonogenic assay, following the protocol described under “Experimental procedures.” Viable cells were seeded at a density of 5000 cells/ml for colony formation and simultaneously treated with different concentrations of NMK-

3-MA, 3-methyladenine; Z, benzyloxycarbonyl; fmk, fluoromethyl ketone; PCNA, proliferating cell nuclear antigen; TUNEL, terminal deoxynucleotidyltransferase-mediated dUTP nick end labeling; DMEM, Dulbecco's modified Eagle's medium; FBS, fetal bovine serum; MTT, 3-(4,5-dimethylthiazol-2-yl)-2,5-diphenyltetrazolium bromide; HRP, horseradish peroxidase; PE, phycoerythrin; PEN-2, Presenilin enhancer 2.

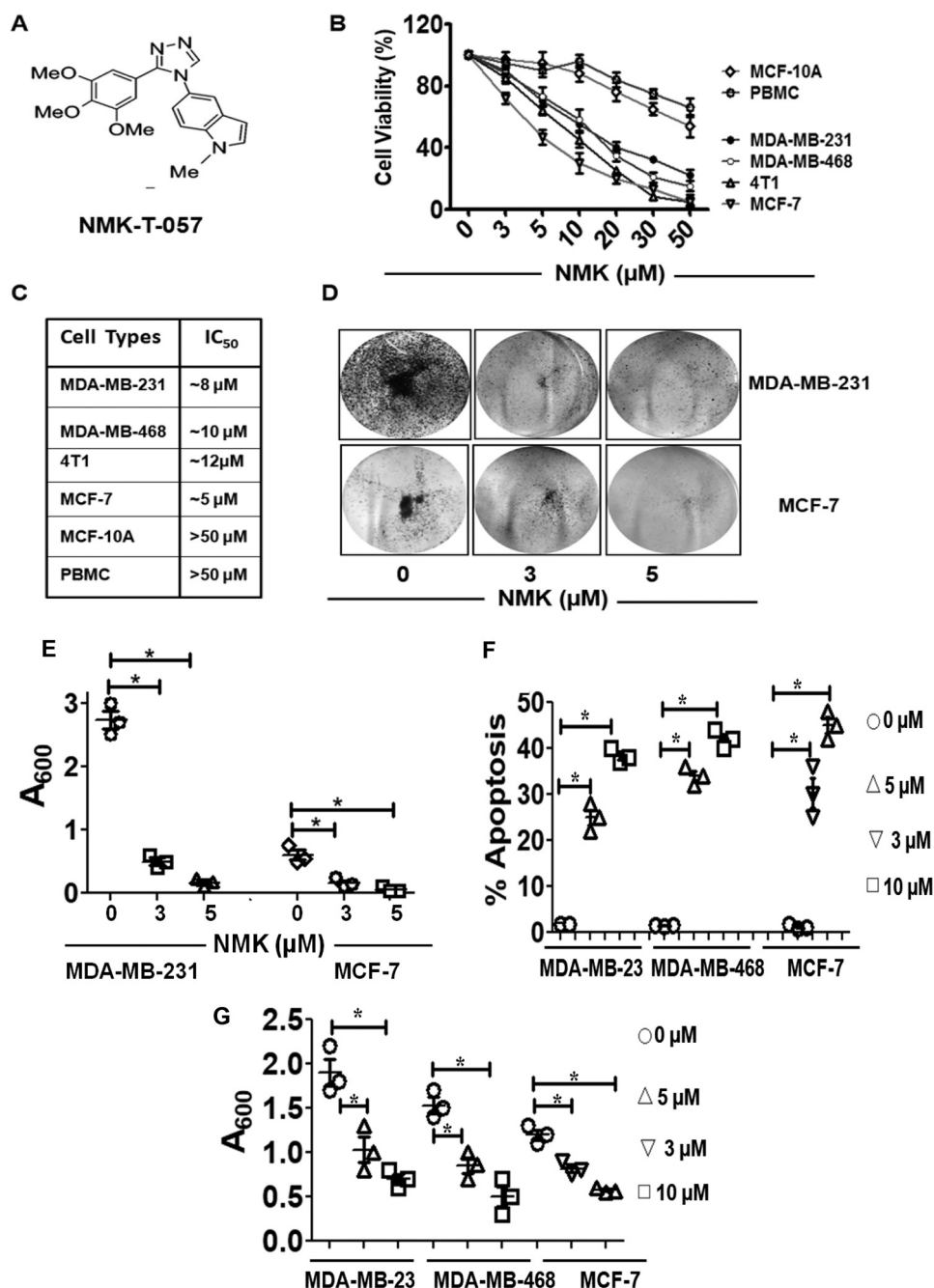


Figure 1. NMK-T-057 inhibits oncogenic potential and induces apoptosis in BC cells. **A**, chemical structure of the novel indolyl triazole derivative NMK-T-057. **B**, effect of NMK-T-057 on viability of BC cells such as MDA-MB-231, MDA-MB-468, 4T1, and MCF-7 and noncancerous cells such as MCF-10A and PBMCs determined by MTT assay after 24 h of treatment. **C**, respective IC₅₀ values of NMK-T-057 on the above-mentioned cell lines. Data are expressed as mean \pm S.E. ($n = 6$); $p < 0.05$. **D**, effect of NMK-T-057 on colony formation of MDA-MB-231 and MCF-7 cells. Colony formation was visualized by staining with crystal violet. The image represents the best of the replicates ($n = 3$). **E**, spectrophotometric analysis of the colony-forming efficiency of MDA-MB-231 and MCF-7 cells (absorbance at 600 nm). Data are expressed as mean \pm S.E. ($n = 3$); $*$, $p < 0.05$ versus control. **F**, apoptosis assay on three different BC cells, MDA-MB-231, MDA-MB-468, and MCF-7, treated with NMK-T-057 (0–10 μM). Data are expressed as mean \pm S.E. ($n = 3$); $*$, $p < 0.05$ versus control (untreated cells). **G**, inhibition of spontaneous transwell migration of MDA-MB-231, MDA-MB-468, and MCF-7 treated with NMK-T-057 (0–10 μM). Data are expressed as mean \pm S.E. ($n = 3$); $*$, $p < 0.05$ versus control (untreated cells). Error bars represent S.E. in respective panels.

T-057 (0–10 μM) from the 2nd to the 6th day. Crystal violet staining of the viable colonies revealed that NMK-T-057 significantly inhibited the colony-forming properties of MDA-MB-231 and MCF-7 cells in a dose-dependent fashion (Fig. 1, **D** and **E**).

To determine the mode of cell death in NMK-treated BC cells we checked the induction of apoptosis by annexin V/pro-

pidium iodide (PI) double staining method using FACS. We observed that treatment of MDA-MB-231, MDA-MB-468, and MCF-7 cells with different concentrations of NMK-T-057 resulted in a dose-dependent induction of apoptosis (Fig. 1**F** and Fig. S1). In the presence of 5 μM compound, the apoptotic population was found to increase 25% from 2% in untreated MDA-MB-231 cells, whereas in MDA-MB-468 cells, the apo-

NMK-T-057 inhibits γ -secretase-mediated Notch activation

ptotic population increased from 1.5 to 35%. Similarly, when treated with 10 μM compound, the apoptotic population increased to 37% in MDA-MB-231 cells and 42% in MDA-MB-468 cells, respectively. Consistent with the cell viability results, MCF-7 cells showed higher responsiveness to NMK-T-057-induced apoptosis. In the presence of 3 μM compound, the apoptotic population increased to 30% as compared with 1.2% in control cells, whereas in the presence of 5 μM compound, the apoptotic population increased to 45%.

Migratory ability of various BC cells in the presence and absence of NMK-T-057 was assessed by Boyden chamber assay. Migratory activities of BC cells were found to be significantly decreased by NMK-T-057 in a dose-dependent fashion (Fig. 1G). In the presence of 5 μM NMK-T-057, the extent of migration was decreased by 1.9- and 1.5-fold for MDA-MB-231 and MDA-MB-468 cells, respectively. Similarly, treatment with 10 μM NMK-T-057 resulted in a decrease of migration by 2.7- and 2.4-fold, respectively. Consistent with our previous results, treatment of MCF-7 cells with NMK-T-057 resulted in drastic inhibition of cell migration. In the presence of 3 and 5 μM NMK-T-057, migration of MCF-7 cells was decreased by 2.7- and 4.8-fold, respectively (Fig. 1G).

After demonstrating the noncytotoxic effect of NMK-T-057 in noncancer cells, we further assessed its toxicity in female Swiss albino mice. NMK-T-057 was injected intraperitoneally in female mice at different doses of (10–100 mg/kg-BW). On the 7th day of i.p. treatment, different hematological and clinical parameters were determined to assess the toxicity of NMK-T-057. We observed that NMK treatments did not significantly affect the red blood cell count or hemoglobin levels in mice compared with the control group. Only minor alterations in the total white blood cell counts were observed, particularly the differential counts for neutrophils and lymphocytes in NMK-treated groups compared with the control group. Additionally, we also observed that NMK-T-057 had no added toxic effects on the liver, as revealed by measuring serum glutamate oxaloacetate transaminase (SGOT), serum glutamate pyruvate transaminase (SGPT), and alkaline phosphatase (ALP) levels in serum from each experimental set. No significant alterations in serum SGOT, SGPT, and ALP levels were observed in NMK-treated mice compared with control mice (Table S1), and all the values fell within the normal range. Thus, consistent with *in vitro* results, NMK-T-057 showed limited toxicity in *in vivo* conditions as well.

NMK-T-057 reverses EMT in TNBCs

Epithelial-to-mesenchymal transition is an important physiological process responsible for the acquisition of migratory and invasive phenotype by BC cells that enhances their ability to invade the surrounding tissues (38). It has been reported that remodeling of the actin cytoskeleton plays an important role in the EMT process (39). Actin stress fibers are found in abundance in mesenchymal cells, whereas few stress fibers are observed in epithelial cells (39). MDA-MB-231 cells, which are known to be highly aggressive and invasive, possess a spindle-shaped morphology similar to the mesenchymal type. Staining the actin cytoskeleton with phalloidin-FITC revealed an organized network of F-actin filaments in the untreated cells. How-

ever, on treatment with sublethal concentrations of NMK-T-057 (3–5 μM), we observed that the mesenchymal morphology of MDA-MB-231 cells was altered to epithelial type accompanied by disruption of the actin stress fibers (Fig. 2A).

We further investigated the status of several EMT markers in NMK-T-057-treated MDA-MB-231 cells. Interestingly, we observed that proteins like vimentin, N-cadherin, and TWIST, which are essential for maintaining the mesenchymal phenotype, were significantly down-regulated by NMK-T-057 in a dose-dependent fashion. Conversely, epithelial markers such as E-cadherin and cytokeratin-19 were also found to be significantly up-regulated in NMK-T-057-treated MDA-MB-231 cells (Fig. 2, B and C). We also observed that the CD44^{high}/CD24^{low} population, responsible for the metastatic potential and stemness properties of BC cells (40, 41), was drastically reduced in the presence of NMK-T-057 (Fig. 2D).

NMK-T-057 attenuates stemness in TNBCs

After confirming the inhibitory effect of NMK-T-057 on mesenchymal markers, we determined the status of aldehyde dehydrogenase (ALDH) 1A, the hallmark of stemness (42, 43), in NMK-treated TNBC cells by FACS (Fig. 3A). We observed that treatment of MDA-MB-231 cells with NMK-T-057 resulted in drastic reduction of the ALDH-positive population from 40% in the control to 21 and 8% in the presence of 3 and 5 μM NMK-T-057, respectively (Fig. 3A).

Cancer stem cells (CSCs) are known to be the driving force of tumorigenesis, and one of the key hallmarks of CSCs is the ability to grow independently of anchorage under serum-free culture conditions, thus resulting in the formation of tumorspheres (44–46). A subpopulation of the basal-like triple-negative MDA-MB-231 cells is reported to form mammospheres when propagated under nondifferentiating culture conditions (47, 48). The cells that escape chemotherapy and result in tumor relapse and acquisition of chemoresistance properties are known as tumor-residual cells or tumor-initiating cells (TICs) (49–51). To determine whether NMK-T-057 can attenuate the stemness properties of TNBC cells, spheroid-forming abilities of untreated and NMK-treated MDA-MB-231 were assessed. A drastic reduction in the number and size of primary spheroids was observed in a dose-dependent fashion due to NMK-treatment. In the presence of 5 μM NMK-T-057, the number of spheroids was reduced from 46 in control to 12 in the treated group. To investigate, whether NMK-T-057 can target the TICs, we prepared secondary spheroids from the untreated and NMK-treated primary spheroids, but the spheroids were propagated in the absence of NMK-T-057. Very interestingly, we observed that even in the absence of NMK-T-057, the number of secondary spheroids derived from NMK-treated primary spheroids was drastically reduced compared with the control (Fig. 3, B and C). Around 32 spheroids were obtained from the control primary spheroids, but only five spheroids were formed from those treated with 5 μM NMK-T-057. Hence, it might be concluded that treatment of TNBCs with NMK-T-057 attenuates the stemness properties of MDA-MB-231 cells.

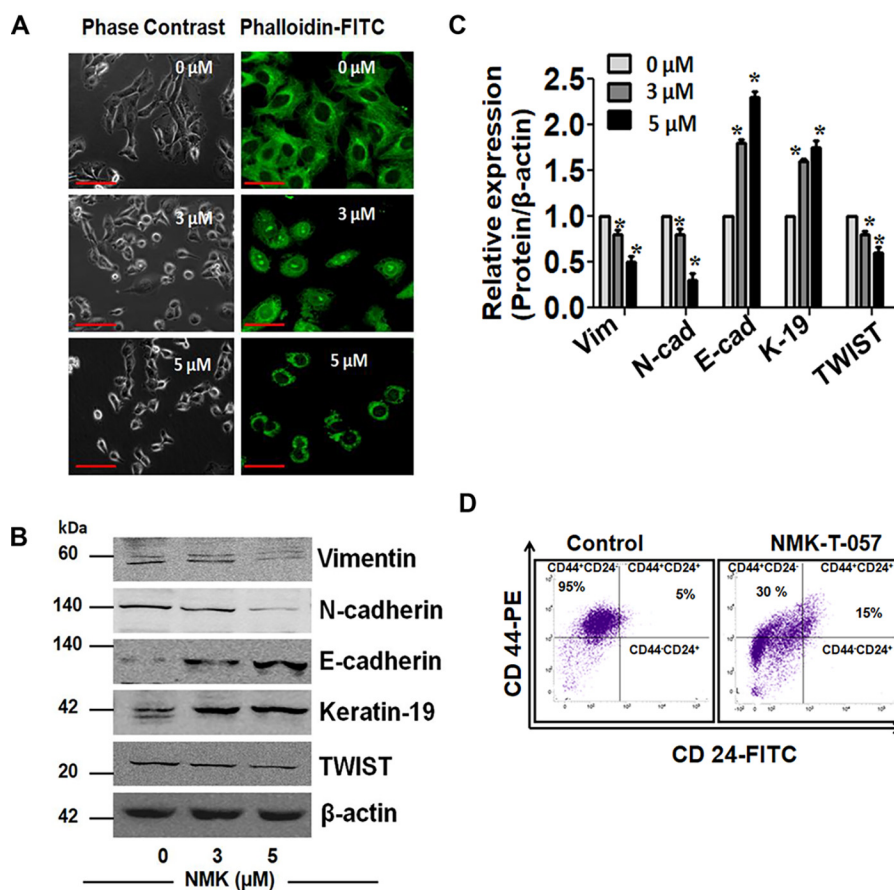


Figure 2. NMK-T-057 induces reprogramming of EMT in BC cells. *A*, stress fiber assay of MDA-MB-231 cells treated with NMK-T-057 (0–5 μ M) for 24 h in two different doses. Cells were stained with FITC-phalloidin to visualize actin stress fibers. Treatment resulted in disruption of actin filaments as compared with untreated controls. The image represents the best of the replicates ($n = 3$). Scale bars, 10 μ m. *B*, Western blot images of vimentin, N-cadherin, E-cadherin, keratin-19, and TWIST in MDA-MB-231 cells treated with NMK-T-057 (0–5 μ M). The blots represent the best of the replicates ($n = 3$). *C*, relative band intensities of vimentin (*Vim*), N-cadherin (*N-cad*), E-cadherin (*E-cad*), keratin-19 (*K-19*), and TWIST in MDA-MB-231 cells treated with NMK-T-057 (0–5 μ M). Data are expressed as mean \pm S.E. ($n = 3$; $p < 0.05$ versus control (untreated cells)). *D*, immunophenotyping with CD24-FITC and CD44-PE in MDA-MB-231 cells treated with 5 μ M NMK-T-057. The data represent the best of the replicates ($n = 3$). Error bars represent S.E. in respective panels.

NMK-T-057 inhibits the progression of tumor residual cells

Malignant breast tumors often consist of a small subset of cell populations known as TICs or CSCs. This subpopulation of BC cells is known to be CD44-positive (CD44^{+/+}) with negligible or no CD24 (CD24^{low/-}) and are responsible for the acquisition of chemoresistance properties and tumor recurrence (47–49). After the treatment with NMK-T-057 (5 and 10 μ M, respectively, for 24 h), the residual viable cells were collected and monitored for their abilities to form colonies and spheroids along with the percentage of CD44^{high}/CD24^{low} population. MDA-MB-231 cells that survived the drug treatment were allowed to grow for 5–7 days, and the above-mentioned properties were monitored. Very interestingly, we observed that the TICs surviving post-drug treatment were highly impaired in colony formation and spheroid formation (Figs. 4, *A–D*). Also, the CD44^{high}/CD24^{low} population was found to be drastically reduced in NMK-treated TICs (Fig. 4*E*).

NMK-T-057 down-regulates Notch/Akt axis in BC cells

Although Notch and Akt signaling pathways have distinct upstream modulators, they were reported to be interrelated in several cancers, including breast cancer (21, 25, 52). It has been reported that Notch-1 activates the phosphatidylinositol 3-ki-

nase/AKT signaling pathway by direct repression of PTEN via the Notch target gene *Hes-1* (25), and inhibition of γ -secretase down-regulates the phosphatidylinositol 3-kinase/Akt pathway in BC cells (52). Moreover, Notch signaling is also known to be the key modulator of stemness in breast cancer (18–20).

Hence, we investigated the status of Notch-1, *Hes-1*, PTEN, and pAkt in MDA-MB-231 cells treated with different concentrations of NMK-T-057 (0–10 μ M). We observed that in the presence of different concentrations of NMK-T-057, expression levels of Notch-1, *Hes-1*, and pAkt were significantly down-regulated, whereas PTEN was up-regulated in a dose-dependent fashion (Fig. 5, *A* and *B*). Thus, it might be predicted that NMK-T-057 targets Notch signaling components in BC cells.

Expression of Notch-1 modulates cytotoxic potential of NMK-T-057 in BC cells

Previous results showed that NMK treatment resulted in the down-regulation of Notch signaling in MDA-MB-231 cells (Fig. 5, *A* and *B*). Hence, we investigated whether Notch expression can modulate the cytotoxicity of NMK-T-057 in BC cells. Interestingly, we observed that siRNA-mediated depletion of Notch-1 enhanced the cytotoxic potential of NMK-T-057 in

NMK-T-057 inhibits γ -secretase-mediated Notch activation

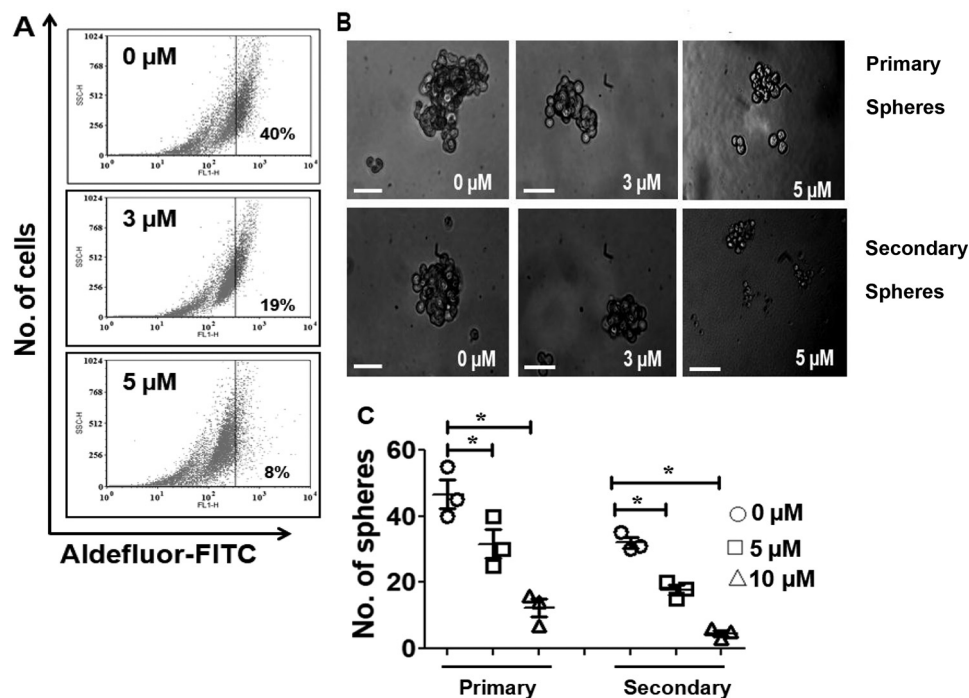


Figure 3. NMK-T-057 inhibits stemness in MDA-MB-231 cells. *A*, ALDFLUOR assay of MDA-MB-231 cells treated with NMK-T-057 (0–5 μ M) for 24 h. The data represent the best of the replicates ($n = 3$). *B*, phase-contrast microscopy images of primary (upper panel) and secondary (lower panel) mammospheres from MDA-MB-231 cells treated with NMK-T-057 (0–5 μ M) for 24 h. Images were taken under 20 \times magnification and represent the best of the replicates ($n = 3$). Scale bar, 100 μ m. *C*, graph showing the number of primary and secondary spheroids versus NMK-T-057 (0–5 μ M). Data are expressed as mean \pm S.E. ($n = 3$); *, $p < 0.05$ versus control (untreated cells). Error bars represent S.E. in respective panels.

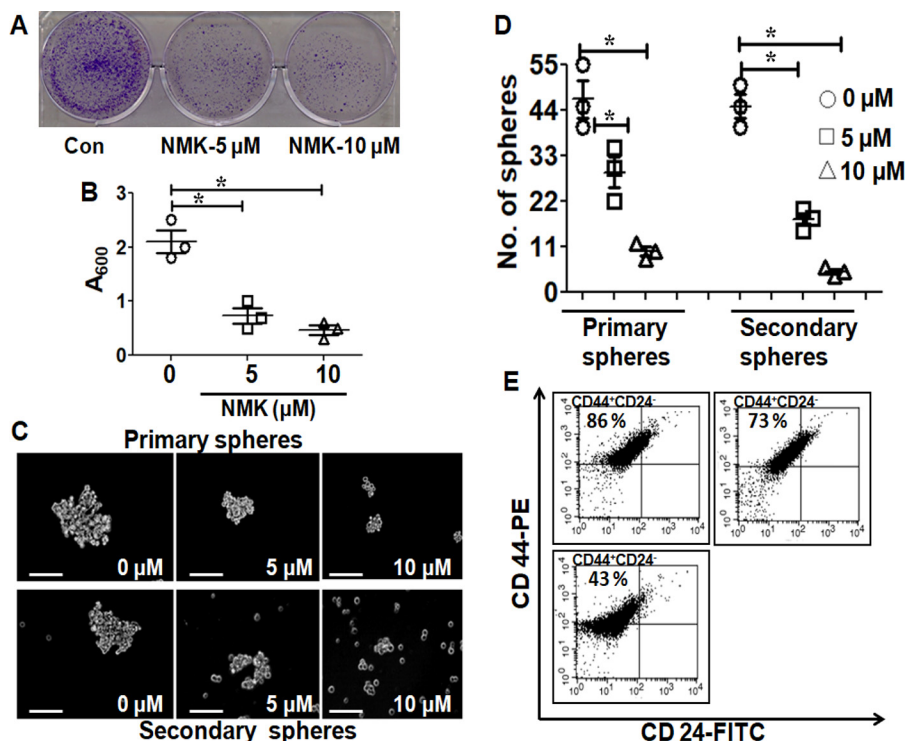


Figure 4. NMK-T-057 inhibits colony-forming ability and stemness in tumor residual cells. *A*, MDA-MB-231 cells were treated with different concentrations of NMK-T-057 (0–10 μ M) for 24 h. The remaining viable cells were collected and subjected to colony formation assay in the absence of the compound. *Con*, control. *B*, spectrophotometric analysis of the colony-forming efficiency of residual cells (MDA-MB-231 at 600 nm). Data are expressed as mean \pm S.E. ($n = 3$); *, $p < 0.05$ versus control. Scale bar, 100 μ m. *C*, phase-contrast microscopy images of primary (upper panel) and secondary (lower panel) mammospheres from residual cells (MDA-MB-231). Images taken under 20 \times magnification and represent the best of the replicates ($n = 3$). *D*, graph showing the number of primary and secondary spheroids from the residual cells. Data are expressed as mean \pm S.E. ($n = 3$); *, $p < 0.05$ versus control (untreated cells). *E*, immunophenotyping with CD24-FITC and CD44-PE in residual cells (MDA-MB-231) treated with 5 μ M NMK-T-057. The data represent the best of the replicates ($n = 3$). Error bars represent S.E. in respective panels.

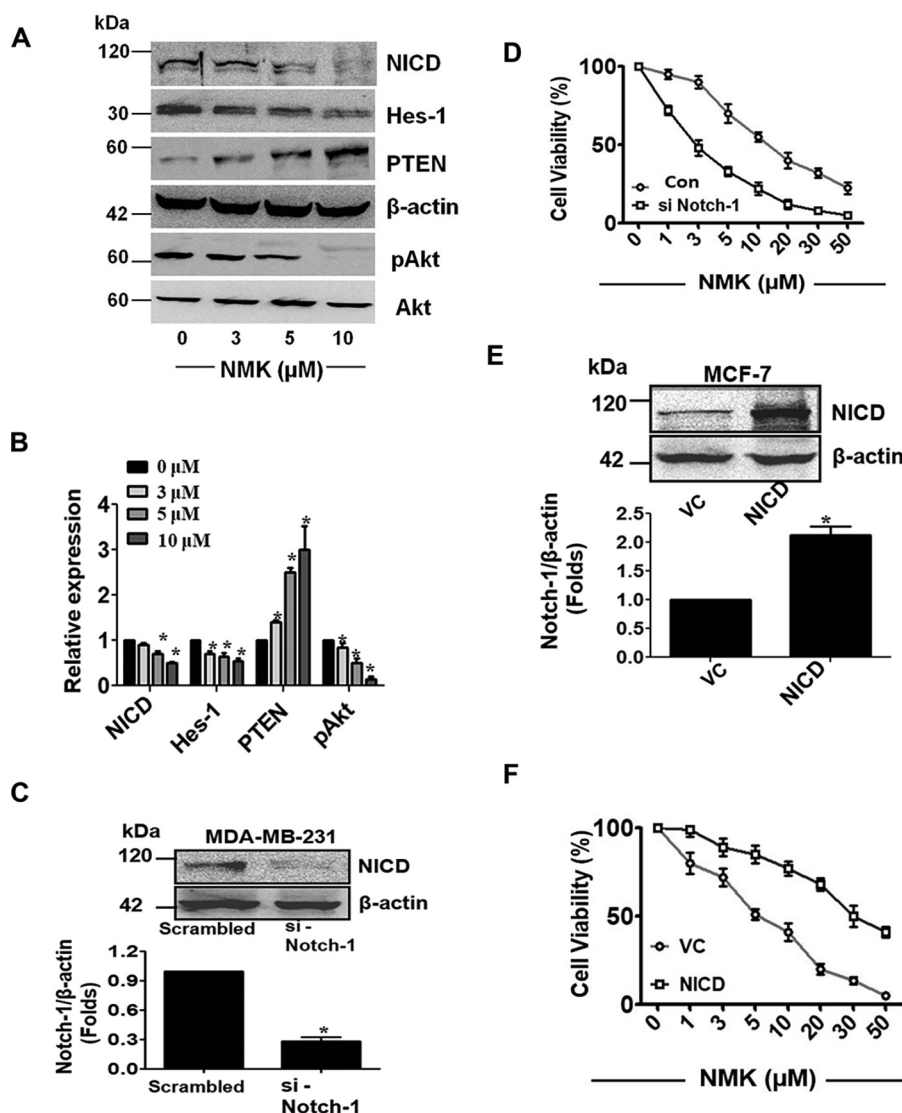


Figure 5. NMK-T-057 inhibits Notch signaling in BC cells. *A*, Western blot images of NICD, Hes-1, PTEN, pAkt, and Akt in MDA-MB-231 cells treated with NMK-T-057 (0–10 μ M). The blots represent the best of the replicates ($n = 3$). *B*, relative band intensities of NICD, Hes-1, PTEN, pAkt, and Akt in MDA-MB-231 cells treated with NMK-T-057 (0–10 μ M). Data are expressed as mean \pm S.E. ($n = 3$); *, $p < 0.05$ versus control (untreated cells). *C*, silencing Notch-1 in MDA-MB-231 cells results in decreased protein expression (~ 0.7 -fold) of NICD as compared with scrambled control. β -Actin was used as the loading control. The blots represent the best of the replicates ($n = 3$). *D*, cell viability assay of MDA-MB-231 cells after transfection with scrambled siRNA (Con) or si-Notch-1 in the presence of different doses of NMK-T-057 (0–50 μ M). Data are expressed as mean \pm S.E. ($n = 6$); *, $p < 0.05$ versus control (untreated cells). *E*, overexpression of NICD in MCF-7 cells. There was an ~ 2 -fold increase in band intensity compared with vector control (VC). The data represent the best of the replicates ($n = 3$). *F*, cell viability assay of MCF-7 cells after transfection with vector control or NICD-GFP in the presence of different doses of NMK-T-057 (0–50 μ M). Data are expressed as mean \pm S.E. ($n = 6$); *, $p < 0.05$ versus control (untreated cells). Error bars represent S.E. in respective panels.

MDA-MB-231 cells (Fig. 5, C and D). In MDA-MB-231 cells transfected with the scrambled siRNA, the IC_{50} of NMK-T-057 was around 10 μ M, whereas in Notch-1 knockout cells, the IC_{50} of NMK-T-057 was reduced to 3 μ M (Fig. 5D). Moreover, to determine the mode of cell death, we investigated the involvement of apoptosis by annexin V-FITC/PI double staining. In the presence of 3 μ M NMK-T-057, only 10% of cells were found to be apoptotic. However, depletion of Notch-1 either by siRNA-mediated transfection or treatment with DAPT, a γ -secretase inhibitor (10 μ M), resulted in the significant induction of apoptosis in MDA-MB-231 cells (Fig. S2). Excessive induction of apoptosis was observed when the Notch-1-depleted cells were further treated with NMK-T-057 (3 μ M). In si-Notch-1-transfected cells treated with 3 μ M NMK-T-057,

$\sim 61\%$ of cells were found to be apoptotic, whereas 7% of cells were necrotic. Similar trends were observed when MDA-MB-231 cells were treated with a combination of DAPT (10 μ M) and NMK-T-057 (3 μ M). A total of 38% of cells were found to be apoptotic, and 12% of cells were necrotic due to this combination treatment (Fig. S2). These results corroborate the previous reports, which suggest that silencing Notch-1 resulted in growth arrest and apoptosis in breast cancer cells (35, 53). It might be concluded that depletion of Notch-1 significantly reduced the malignant properties of MDA-MB-231 cells and made them sensitive to NMK-T-057 treatment. Also, involvement of any other target for NMK-T-057, which might become functional in the absence of Notch-1, could not be ruled out.

NMK-T-057 inhibits γ -secretase-mediated Notch activation

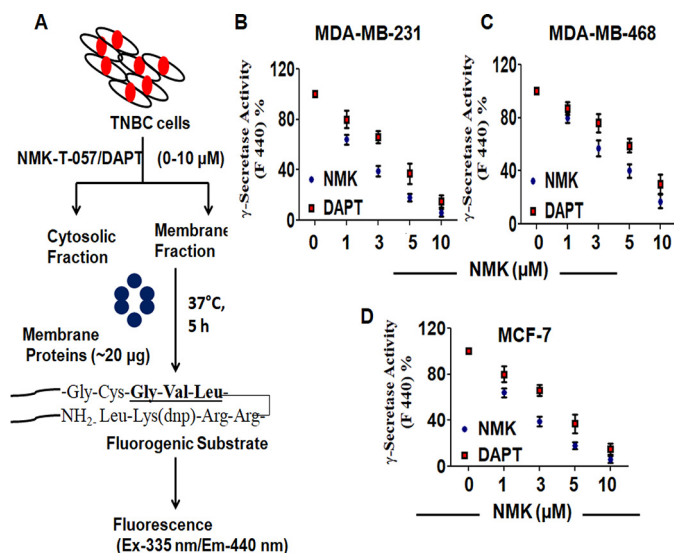


Figure 6. NMK-T-057 inhibits γ -secretase activity in BC cells. A, a diagrammatic representation indicating the determination of γ -secretase activity in BC treated with NMK-T-057 using a fluorogenic substrate. B–D, determination of comparative dose-dependent inhibition of γ -secretase activity by NMK-T-057 and DAPT in MDA-MB-231, MDA-MB-468, and MCF-7 cells, respectively. Data are expressed as mean \pm S.E. ($n = 3$); *, $p < 0.05$ versus control (untreated cells). Ex, excitation; Em, emission. Error bars represent S.E. in respective panels.

Conversely, transfection of MCF-7 cells with active NICD-GFP plasmid impaired the cytotoxic potential of NMK-T-057 (Fig. 5, E and F). When MCF-7 cells were transfected with the empty vector and treated with NMK-T-057, the IC_{50} was around $5 \mu M$, but in the cells transfected with NICD-GFP plasmid, the IC_{50} value drastically increased to around $30 \mu M$. This is a very significant result that clearly indicates that expression levels of intracellular Notch-1 modulate the cytotoxic potential of NMK-T-057 in BC cells.

NMK-T-057 inhibits the activity of γ -secretase enzyme in TNBC cells

The enzyme γ -secretase plays an important role in the activation and nuclear translocation of Notch-1 (23, 24). The PSEN-1 component of γ -secretase catalyzes S3 cleavage of Notch precursor to release the activated NICD into the cytosol (24). Because the mechanism of action of NMK-T-057 was found to be quite similar to that of DAPT, we examined whether NMK-T-057 could inhibit γ -secretase activity in TNBC cells. We measured γ -secretase activity in MDA-MB-231 and MDA-MB-468 cells using the fluorogenic substrate NMA-Gly-Cys-Gly-Val-Leu-Leu-Lys(dnp)-Arg-Arg-NH₂ trifluoroacetate, which mimics the Gly-Val-Leu sequence required for S3 cleavage (54) (Fig. 6A). We observed that both NMK-T-057 and DAPT treatment resulted in a dose-dependent inhibition of γ -secretase activity in MDA-MB-231 and MDA-MB-468 cells as well as MCF-7 cells (Fig. 6, B–D). Thus, this result suggests that NMK-T-057 down-regulates the expression of active Notch-1 by inhibiting γ -secretase activity.

NMK-T-057 binds to the interface of Nicastrin and APH-1 subunits of γ -secretase complex

To identify the putative binding site of NMK-T-057 and DAPT on γ -secretase, molecular docking was performed using

the software UCSF Chimera 1.11 and AutodockTools 1.5.6. DAPT is known to bind to PSEN-1 subunit (55). Our blind docking studies suggest that DAPT binds at the interface of the subunits PSEN-1 (subunit B) and APH-1 (subunit C) (Fig. 7, A–C). The binding pocket was found to be stabilized by hydrophobic interactions and van der Waals interactions between DAPT and selective amino acids of these two subunits. The C16, C17, and C18 atoms of the *t*-butyl methoxy group of DAPT were involved in strong alkyl type hydrophobic interaction with Ala (C39), Val (B412), Leu (B415), Val (C36), Leu (C35), Ile (C127), and Ile (C128) (A, chain Nicastrin; B, chain Presenilin1; C, chain APH1A; D, chain Presenilin2). A strong interaction was observed between the π orbital electron located at the benzene ring of DAPT and that of the benzene ring of phenylalanine (B411) and the alkyl chain of isoleucine (B411). Moreover, the valine residues (C131 and C32) of APH-1 stabilize the complex with van der Waals attractive forces (Fig. 7C). The estimated binding energy was found to be -7 kcal/mol.

We followed the same procedure to identify the putative binding site of NMK-T-057 on γ -secretase enzyme complex. Very interestingly, we observed that NMK-T-057 binds to γ -secretase complex at 4.2 \AA apart from DAPT-binding site, and the binding pocket is a loop made up of Nicastrin and APH-1 subunits (Fig. 7, D and E). The protein–ligand complex was found to be stabilized by H-bonding, hydrophobic interactions, and van der Waals interactions. Docking studies revealed that H1 and C18 atoms of NMK-T-057 were forming H-bonds with Tyr (C119), Ser (A683), and Pro (C16) residues. Among different types of hydrophobic interactions, π -alkyl type interaction contributes the most. The π electron-rich aromatic rings of NMK-T-057 were interacting with alkyl chains of Leu (C20), Ile (A690), Val (C176), Ala (C228), and Ala (C232) residues. The π electrons present in the benzene ring of NMK-T-057 were found to interact with the C–H σ electron of Leu (C169), whereas the π electrons of the 1,3,4-triazole ring of NMK-T-057 interact with the π electrons of the benzene ring of the phenylalanine (C173) residue (Fig. 7F). The estimated binding energy was found to be -8 kcal/mol. Detailed information of the interactions of NMK-T-057 and DAPT with γ -secretase complex has been documented in Table S2.

NMK-T-057 induces autophagy in BC cells

Previously, it has been reported that inhibition of Notch signaling induces autophagy in BC cells (36, 37). Autophagy is characterized by the appearance of stress vacuoles and recruitment of the microtubule-associated protein light chain 3 (LC3) to autophagosomes as LC3-I and subsequent formation of LC3-II (56). To investigate the induction of autophagy in NMK-treated MDA-MB-231 cells, we quantified the autophagic stress vacuoles by flow cytometry and confocal microscopy using the fluorescent dye monodansylcadaverine (MDC) that specifically stains autophagosomes. MDA-MB-231 cells were treated with 3 and $5 \mu M$ NMK-T-057, which are concentrations that are less than the IC_{50} concentration but significantly inhibited γ -secretase activity, and with a sublethal dose of DAPT ($10 \mu M$), at which significant inhibition of γ -secretase had been observed. Flow cytometry studies revealed that treatment of MDA-MB-231 cells with NMK-T-057 resulted in a

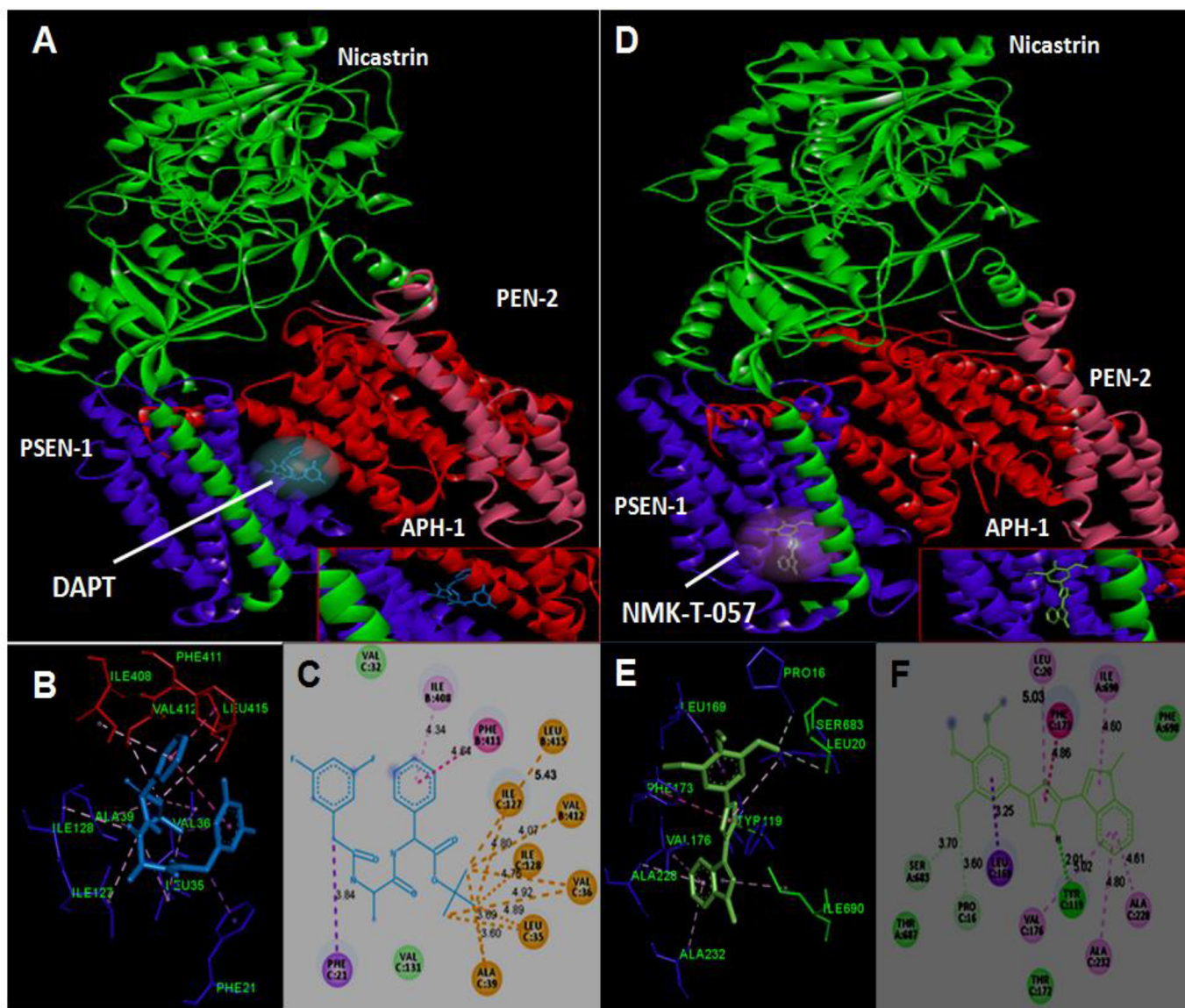


Figure 7. *In silico* docking study of the binding of DAPT and NMK-T-057 to γ -secretase subunits. To identify the putative binding site of the novel compound and DAPT on γ -secretase tetramer, molecular docking was performed using UCSF Chimera 1.11 and AutodockTools 1.5.6. A–C, binding interactions of DAPT with the multisubunit enzyme γ -secretase. D–F, binding interactions of NMK-T-057 with the multisubunit enzyme γ -secretase.

significant induction of autophagy as evident from the increase in the MDC-positive population from 2.8% in control to 20 and 28% in the presence of 3 and 5 μ M NMK-T-057, respectively. Very interestingly, treatment of MDA-MB-231 cells with DAPT also resulted in the increase of the MDC-positive population to 25% compared with the control. Administration of the autophagy inhibitor 3-methyladenine (3-MA) completely attenuated the MDC-positive population in the treatment sets (Fig. 8A and Fig. S3). This result was further validated by confocal microscopy, which showed a similar pattern of autophagy induction in MDA-MB-231 cells treated with both NMK-T-057 and DAPT (Fig. 8B). Autophagy-inducing proteins like Beclin-I and LC3-I/II were also found to be significantly up-regulated in MDA-MB-231 cells treated with NMK-T-057 and DAPT (Fig. 8C), a very interesting observation suggesting that pharmacological inhibition of γ -secretase-mediated Notch activation resulted in the induction of autophagic responses.

NMK-T-057 induces autophagy-dependent apoptosis in BC cells

Although apoptosis and autophagy are two different physiological processes, it has been reported that these two events might be interdependent or mutually independent (57). Hence, we investigated in detail whether these two processes play a part in NMK-mediated cytotoxicity independently or whether they are interdependent. First, we monitored time-dependent induction of both autophagy and apoptosis in NMK-treated MDA-MB-231 cells. Within 6 h of treatment, a significant increase in autophagic flux was observed, maximum autophagic response was observed after 12 h, and this response was found to be decreased after 24 h. However, no significant apoptotic population was observed after 6 and 12 h of treatment. The apoptotic population was found to be significantly increased only after 24 h of treatment (Fig. 8D and Fig. S4). The

NMK-T-057 inhibits γ -secretase-mediated Notch activation

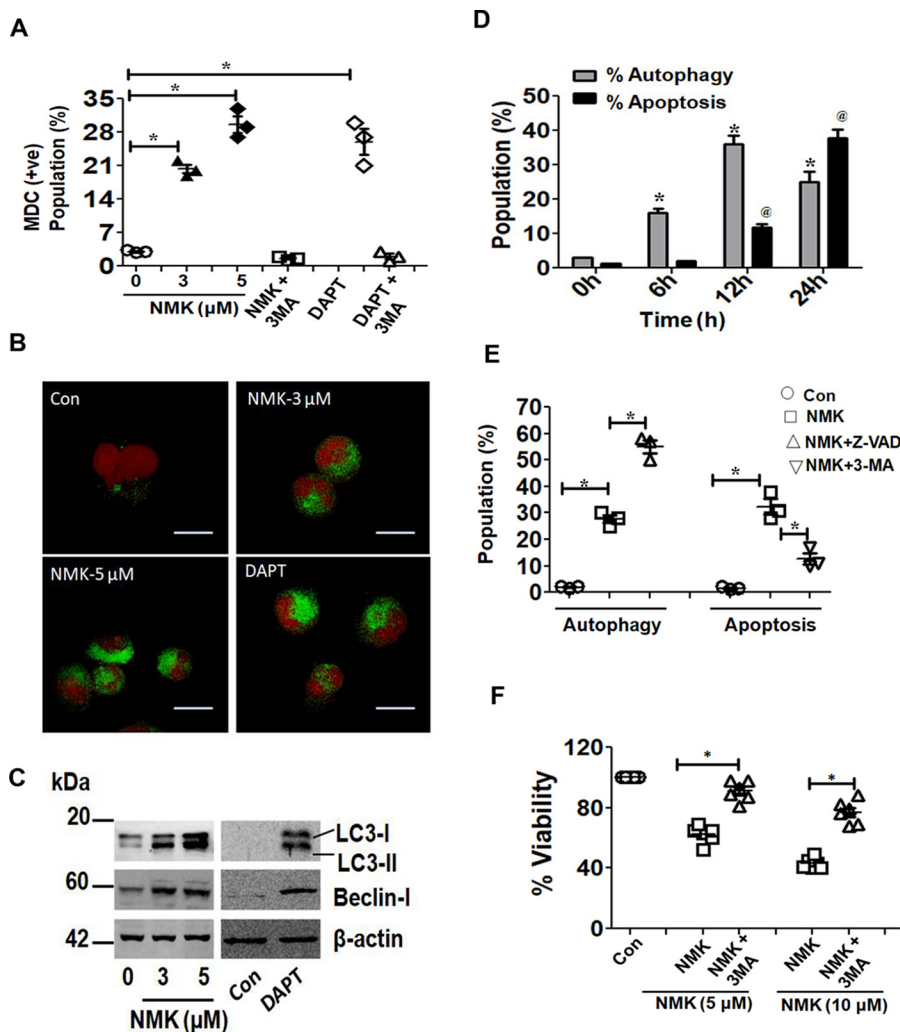


Figure 8. NMK-T-057 induces autophagy-dependent apoptosis in BC cells. *A*, induction of autophagy in MDA-MB-231 cells treated with NMK-T-057 (0–5 μ M), DAPT (10 μ M), and autophagy inhibitor 3-MA (500 μ M) as determined by FACS using the fluorescent dye MDC. Data are expressed as mean \pm S.E. ($n = 3$); *, $p < 0.05$ versus control (untreated cells). +ve, positive. *B*, confocal images of autophagic vacuoles in MDA-MB-231 cells treated with NMK-T-057 (0–5 μ M) and DAPT (10 μ M) after staining with MDC. The images represent the best of the replicates ($n = 3$). Scale bar, 10 μ m. *C*, Western blot analysis of LC3-I/LC3-II and Beclin-1 in MDA-MB-231 cells treated with NMK-T-057 (0–5 μ M) and DAPT (10 μ M). The blots represent the best of the replicates ($n = 3$). *D*, time-dependent induction of autophagy and apoptosis in MDA-MB-231 cells treated with 5 μ M NMK-T-057. Data were collected by staining with MDC and annexin V-FITC using FACS after intervals of 6, 12, and 24 h. Data are expressed as mean \pm S.E. ($n = 3$); *, $p < 0.05$ versus control (untreated cells). *E*, cross-inhibitor study of autophagy and apoptosis in MDA-MB-231 cells treated with 5 μ M NMK-T-057, preincubated with the autophagy inhibitor 3-MA and apoptosis inhibitor Z-VAD-fmk. Data are expressed as mean \pm S.E. ($n = 3$); *, $p < 0.05$ versus control (untreated cells). *F*, cell viability assay of MDA-MB-231 cells treated with NMK-T-057 (5 and 10 μ M) and NMK-T-057 + 3-MA. Data are expressed as mean \pm S.E. ($n = 3$); *, $p < 0.05$ versus NMK-T-057 treated cells. Con, control. Error bars represent S.E. in respective panels.

results clearly indicate that autophagy precedes apoptosis in NMK-treated cells.

Second, to further investigate whether these two events are parallel or interdependent, we administered specific inhibitors for autophagy and apoptosis and then evaluated the effect on each other (Fig. 8E and Fig. S5). Very interestingly, we observed that administration of Z-VAD-fmk, an apoptosis inhibitor, increased the autophagic population from 27 to 55% in NMK-treated MDA-MB-231 cells, but administration of the autophagy inhibitor 3-methyladenine significantly reduced the apoptotic population (Fig. 8E and Fig. S5). A small population of cells were also found to be necrotic due to NMK treatment (~5%) but were absent in the presence of the autophagy inhibitor 3-methyladenine. Furthermore, it was also observed that application of 3-methyladenine restored the viability of NMK-

treated MDA-MB-231 cells to a significant extent (Fig. 8F). Cumulatively, these results indicate that autophagy was induced as an early event in NMK-treated cells and finally led to apoptosis-mediated cell death.

NMK-T-057 inhibits the progression of breast tumors in 4T1 xenograft model

After *in vitro* confirmation of the anticancer potential of NMK-T-057, we further investigated its efficacy under *in vivo* conditions using 4T1–BALB/c syngeneic pair model. Female BALB/c mice carrying palpable tumors formed of 4T1 cells at their mammary fat pads were treated with different concentrations of NMK-T-057 (0–50 mg/kg-BW) for 3 weeks. Significant reduction in tumor volume was observed in the presence of NMK doses of 25 and 50 mg/kg-BW. A lesser extent of tumor

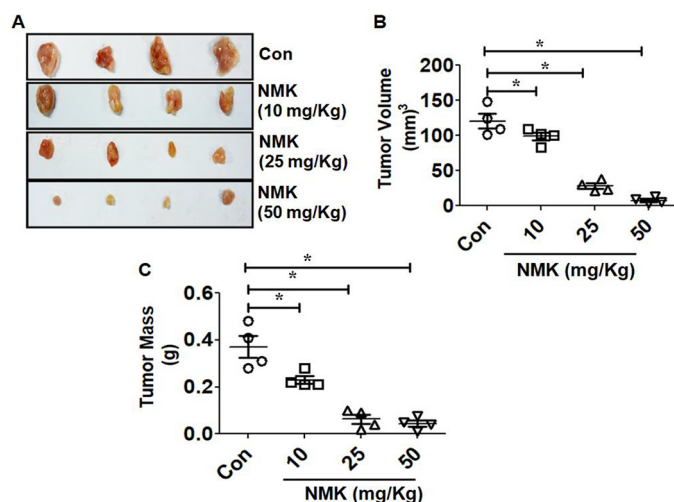


Figure 9. NMK-T-057 reduces tumor volume and mass in 4T1 cell-induced tumor in BALB/c mice. *A*, comparative representative photographs of tumor volume in control and NMK-T-057 (10, 25, and 50 mg/kg-BW)-treated BALB/c mice after 15 days of treatment. *B*, graph showing the reduced tumor volume in treated groups as compared with control tumor (*Con*), respectively. *C*, graph representing dissected tumor mass of control and NMK-T-057 (10, 25, and 50 mg/kg-BW)-treated tumors from BALB/c mice. All data are expressed as mean \pm S.E. ($n = 6$); *, $p < 0.05$ versus control. Error bars represent S.E. in respective panels.

inhibition was observed in the presence of 10 mg/kg-BW NMK (Fig. 9, *A* and *B*). Subsequently, a significant reduction of tumor mass was observed in a dose-dependent manner in treated groups (Fig. 9*C*). Moreover, by immunohistochemistry and immunofluorescence studies, we confirmed the reduction of proliferating cells in NMK-treated tumors (PCNA-staining) and induction of apoptosis as determined by TUNEL assay and caspase-3 staining. A dose-dependent decrease in PCNA-positive cells and increase in TUNEL/caspase-3-positive cells were observed in NMK-treated tumors (Fig. 10). Thus, cumulatively, the results indicate antitumor efficacy of NMK-T-057 in the 4T1 xenograft tumor model.

NMK-T-057 down-regulates Notch expression in tumor samples

Because a significant down-regulation of active Notch (NICD) was observed in NMK-treated BC cells, we further monitored the expression of NICD in NMK-treated tumors. We observed a drastic reduction in NICD expression in NMK-treated tumors (Fig. 11, *A* and *B*). Expression of NICD was found to be significantly reduced, especially at those concentrations of NMK-T-057 that effectively inhibited tumor progression.

Discussion

The increasing incidence of breast cancer has become a life-threatening risk to the female population globally. The mortality rate in the female population of India due to BC has also increased significantly in recent years (3, 4). Notch signaling, an evolutionarily conserved pathway, is known to play a pivotal role in a variety of physiological processes such as cell-cell communication, cellular proliferation, differentiation, and embryogenesis (58). Despite important cellular functions, Notch signaling was also found to be highly deregulated in sev-

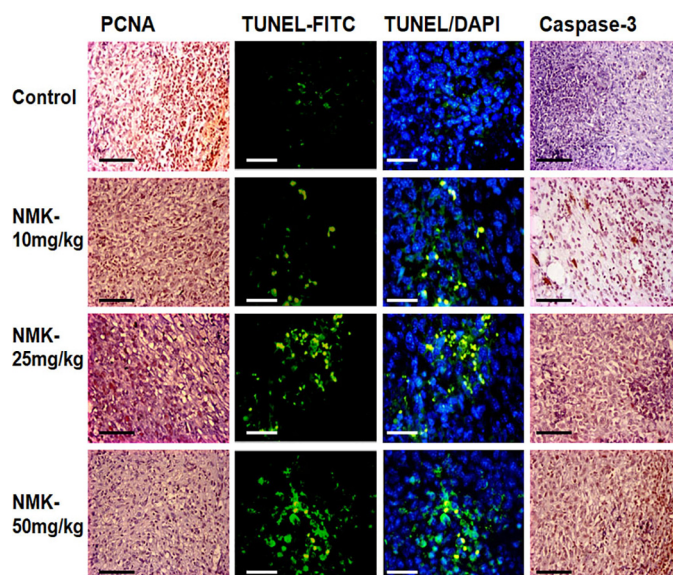


Figure 10. NMK-T-057 inhibits proliferation and induces apoptosis in control and treated tumor in BALB/c mice. The photographs show the immunohistochemistry of PCNA and caspase-3 and immunofluorescence of TUNEL assay in control and NMK-T-057 (10, 25, and 50 mg/kg-BW)-treated tumors. The photographs represent the best of the replicates ($n = 3$). Scale bars, 10 μ m.

eral human malignancies, including breast cancer (8–11), and responsible for the acquisition of drug resistance and stemness in breast cancer (12–17). Thus, developing novel therapies targeting the Notch signaling pathway at different levels of the cascade is of growing interest in the development of anticancer therapeutics against breast cancer (19, 21, 22). To date, several strategies of Notch inhibition have been reported, including antibodies against Notch receptors or ligands, GSIs, and siRNA, but the most effective mode of inhibition was shown to be the application of GSIs (27). The multisubunit enzyme γ -secretase catalyzes the critical step of Notch activation, thus releasing activated NICD into the cytosol (24). Hence, inhibition of the γ -secretase-mediated activation of Notch signaling might be an effective therapeutic approach to inhibit the growth and progression of cancer cells. Moreover, GSIs are also known to suppress the stem cell characteristics of breast cancer cells, including TNBCs (59).

In our study, we have observed that the indolyl triazole derivative NMK-T-057 significantly reduced the viability and colony-forming property of several types of BC cells, with negligible cytotoxicity toward the noncancerous cells. Moreover, this compound also induced apoptosis and inhibited the migratory properties of several types of BC cells. The drastic change in morphology of BC cells such as MDA-MB-231 treated with NMK-T-057 further encouraged us to investigate its effect on EMT and stemness. Very interestingly, we observed that NMK treatment of MDA-MB-231 cells resulted in the reprogramming of EMT and simultaneously inhibited the stemness, which is a positive indication of better tumor prognosis and reduction of the risk of future tumor relapse. Further investigations revealed that NMK-T-057 targets the Notch-1/Akt axis in TNBC cells and that its cytotoxic potential is related to the presence or absence of intracellular active NICD.

NMK-T-057 inhibits γ -secretase-mediated Notch activation

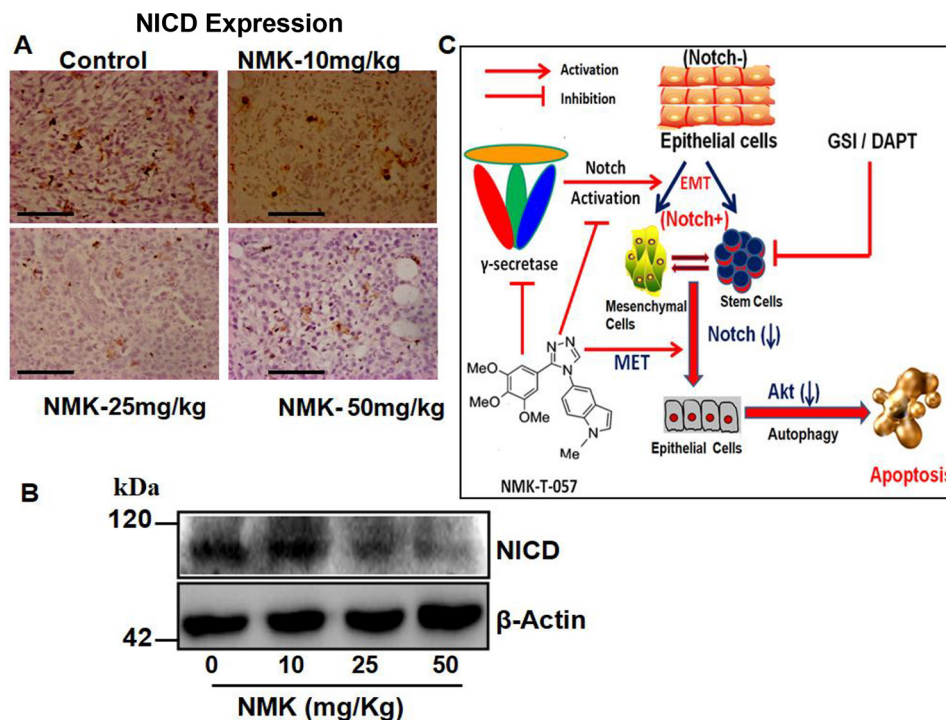


Figure 11. NMK-T-057 down-regulates active Notch (NICD) expression *in vivo* in 4T1-BALB/c tumors. A, photographs representing immunohistochemistry of NICD in control and NMK-T-057 (10, 25, and 50 mg/kg-BW)-treated tumors. The photographs represent the best of the replicates ($n = 3$). Scale bars, 10 μ m. B, Western blot of NICD in tumors of control and treated groups. C, schematic representation of the mechanism of action of NMK-T-057 in breast cancer.

Down-regulation of Notch signaling could be achieved by the pharmacological inhibition of γ -secretase by γ -secretase inhibitors or GSIs, which are reported to show significant anticancer properties against several carcinomas, including breast, and a few of them have also entered clinical trials (26, 27). Because NMK-T-057 can efficiently down-regulate Notch signaling, we investigated the effect of this compound on γ -secretase activity in BCs. Very interestingly, we observed that NMK-T-057 effectively inhibits the activity of γ -secretase in MDA-MB-231 and MDA-MB-468 cells, and the extent of inhibition is slightly better than the commercially available γ -secretase inhibitor DAPT. Furthermore, docking studies revealed that NMK-T-057 has a binding site on γ -secretase complex, consisting of a loop composed of Nicastrin and APH-1 subunits.

Accumulating experimental evidence suggests a correlation between induction of autophagy and inhibition of Notch signaling (11, 36, 60), and particularly down-regulation of Notch-1 triggers autophagy-mediated cell death in cancer cells (36, 37). However, there has been no report so far about the induction of autophagy by GSIs. Henceforth, we monitored whether GSIs such as NMK-T-057 and DAPT can induce autophagy in BCs. We observed that both NMK-T-057 and DAPT induced significant autophagy in MDA-MB-231 cells along with drastic up-regulation of inducing proteins like Beclin-1 and LC3-I. There have been several reports that have suggested that autophagy might be the inducer of apoptosis in cancer cells treated with certain anticancer drugs (61–63). Moreover, excessive autophagy is also known to cause cell death via necroptosis, a process known as autosis (64, 65). To investigate whether autophagy plays any role in NMK-induced apoptosis, we performed time kinetics and cross-inhibitor studies to

determine the interdependence between these two processes. Both the results indicated that autophagy is an event that precedes apoptosis in NMK-treated cells. All these results indicate that the triazole derivative NMK-T-057 has the potential to suppress Notch signaling in BCs, by inhibiting the activity of γ -secretase complex, via direct binding to the interface of Nicastrin and APH-1 subunits. Another interesting finding of this study is that GSIs such as DAPT and NMK-T-057 induce autophagy in BCs as an early event, which is then followed by apoptosis as the cell death mechanism.

Small-molecule inhibitors of γ -secretase or GSIs were initially designed to prevent the accumulation of amyloid plaques in Alzheimer's disease. However, considering the importance of Notch signaling in a variety of aggressive cancers, GSIs have been repurposed to block the enzyme activity as a promising approach to treat cancer (59, 66). Depending on their ability to directly bind the active site of the enzyme, GSIs can be broadly classified into transition-state inhibitors, which can competitively bind to the active site of the enzyme, and nontransition-state analogues, which bind to sites other than the active site (67). DAPT is an early-generation nontransition-state inhibitor that was found to be effective against several carcinomas, including breast cancer, and is also known to inhibit the metastasis of breast cancer to the brain (68–71). Later, several small-molecules (*e.g.* LY411575, LY450139, RO4929097, BMS906024, and MK0752) were developed and have been tested in phase I/phase II clinical trials (67). In this context, we have observed that NMK-T-057 exhibited significant inhibitory effects on γ -secretase activity, impaired EMT and stemness in BCs, and induced profound cytotoxicity against BC under *in vitro* and *in vivo* conditions. Hence, NMK-T-057, hav-

ing a unique intracellular target, can be a good drug candidate against BC. The mode of action of NMK-T-057 against BC has been demonstrated in Fig. 11C.

Experimental procedures

Dulbecco's modified Eagle's medium (DMEM) (supplemented with 1 mM L-glutamine), fetal bovine serum (FBS), penicillin-streptomycin solution, amphotericin B, and hydrocortisone were purchased from HyClone (GE Healthcare). Trypsin-EDTA and Boyden chambers were purchased from HiMedia, India. MDC, trypan blue, PI, dimethyl sulfoxide (DMSO), Ficoll-Hypaque, phalloidin-FITC, and γ -secretase assay kits were purchased from Sigma. 3-(4,5-Dimethylthiazol-2-yl)-2,5-diphenyltetrazolium bromide (MTT), annexin V-FITC, Lipofectamine 2000, and Opti-MEM, were obtained from Thermo Fischer. Control scrambled siRNA (sc-44230), si-Notch-1 (sc-36095), mouse monoclonal anti- β -actin antibody (sc-47778; C4), mouse monoclonal anti-Bcl-1 (sc-48341; E8), mouse monoclonal anti-vimentin (sc-6260; V9), mouse monoclonal anti-E-cadherin (sc-71009), mouse monoclonal anti-N-cadherin (sc-59987; 13A9), rabbit polyclonal anti-TWIST (sc-15393), mouse monoclonal anti-HES1 (sc-166410; E-5), mouse monoclonal anti-PCNA (sc-56), and mouse monoclonal anti-PTEN (sc-7974; A2B1) antibodies were purchased from Santa Cruz Biotechnology (Santa Cruz, CA). Rabbit monoclonal cleaved Notch-1 (4147; D3B8), rabbit monoclonal anti-cleaved caspase-3 (9661), rabbit monoclonal anti-LC3 antibody (catalogue number 3868; clone-D11), rabbit monoclonal anti-phospho-Akt (Ser-473) (4060; D9E), and rabbit monoclonal anti-Akt (4691; C67E7) antibodies were purchased from Cell Signaling Technology. The Qproteome Cell Compartment kit was purchased from Qiagen. The Bradford protein estimation kit, goat anti-mouse IgG horseradish peroxidase (HRP), and rabbit anti-goat IgG-HRP were purchased from Genei (India). All other reagents and chemicals were analytical grade and were purchased from Sisco Research Laboratories (India). NMK-T-057 (Fig. 1A) was provided by the laboratory of Dr. Dalip Kumar, and the synthesis of this compound has been published previously (29).

Cell culture and maintenance

Normal breast epithelial cells (MCF-10A cells) were cultured in complete DMEM/F-12 (50:50, v/v) growth medium supplemented with 10% FBS, 100 units/ml penicillin, 100 μ g/ml streptomycin, 0.5 μ g/ml hydrocortisone, 10 μ g/ml insulin, 100 ng/ml cholera toxin, 10 ng/ml epidermal growth factor, and 1% (w/v) L-glutamine. MDA-MB-231, MDA-MB-468, 4T1, and MCF-7 cells were supplemented with 10% FBS, 100 units/ml penicillin, and 100 μ g/ml streptomycin at 37 °C in a humidified chamber.

Human blood collection from adult healthy volunteers and experiments with human peripheral blood mononuclear cells were approved by the Institutional Bioethics Committee for animal and human research studies, University of Calcutta, following the Code of Ethics of the World Medical Association (Declaration of Helsinki) for experiments involving humans. Human PBMCs were isolated from the whole blood of healthy adult donors using the density gradient Ficoll-Hypaque

method. Whole blood collected from the donor was mixed with an equal volume of Ficoll-Hypaque. The mixture was then centrifuged at $400 \times g$ for 30 min at room temperature, and PBMCs were collected from the plasma/Ficoll-Hypaque interphase. Isolated PBMCs were washed in sterile PBS and resuspended in RPMI 1640 complete medium supplemented with 10% FBS.

Animals

Female Swiss albino and BALB/c mice (body weight, 20 ± 22 g) from Central Research Institute and Bose Institute, Kolkata, India, respectively, were housed in polypropylene cages under standard laboratory conditions of $50 \pm 10\%$ relative humidity, 22 ± 2 °C temperature, and 12-h/12-h light-dark cycle for 10 days prior to commencement of experiments. All animal experiments were conducted according to the approval and guidelines of the Institutional Animal Ethical Committee, Government of India (registration numbers 885/ac/05/CPC-SEA and IAEC/BI/114/2018). Mice were maintained with water and standard diet *ad libitum*. They were acclimatized to laboratory conditions 10 days before commencement of experiments and fasted overnight before experimentation. Food was restored after injections but withdrawn 6 h prior to sacrifice and analysis. Effects of NMK-T-057 on different pathophysiological parameters of mice were assessed following published protocols (72).

Cytotoxicity assays in mice and treatment strategies

Because NMK-T-057 is poorly soluble in water, a suitable vehicle is required to dissolve and deliver it intraperitoneally. Among different techniques available, emulsion is the safest and most widely used technique for the administration of water-insoluble drugs (73). We have used Food and Drug Administration-approved, commercially available excipients like polysorbate-20 (as surfactant), propylene glycol (as cosurfactant), and castor oil to make oil/water (oil/water emulsion) (73) of NMK-T-057. In short, 12 mg of the drug was dissolved in a mixture of 150 mg of castor oil and 300 mg of polysorbate-20 by vortexing for 10 min. Then 50 μ l of propylene glycol was added and mixed thoroughly by vortexing for 15 min. Finally, 500 μ l of Milli-Q water was added dropwise with continuous mixing to make the oil/water emulsion. This emulsion was administered intraperitoneally in female Swiss albino mice at different NMK-T-057 doses (10–100 mg/kg-BW).

For the toxicity study, five mice kept as controls were injected with the oil emulsion. The rest of the mice were injected with NMK doses (25–100 mg/kg-BW in oil emulsion; $n = 5$). All animals, including control groups, were subjected to intraperitoneal injection daily up to 7 days. At the end of the experiment, animals were weighed and sacrificed for further analysis.

The immediate toxic impact of drugs can be elucidated from interactions with different blood cells *in vivo*. Prior to determining the effects of NMK doses on cancer cells, it was imperative to assess whether the compound conferred toxicity on hematological parameters of normal animals. Effects of NMK on blood parameters like red blood cell, white blood cell (total and differential), and hemoglobin content were determined in normal mice. A 7-day treatment schedule was maintained at equivalent doses of 25 and 50 mg/kg in two sets. Serum was

NMK-T-057 inhibits γ -secretase-mediated Notch activation

isolated from the blood of control and NMK-treated mice by centrifugation at $2000 \times g$ for 5 min. SGPT, SGOT, and ALP were estimated using Robonik[®] (India) following the manufacturer's protocol.

MTT assay

Different TNBC cells such as MDA-MB-231, MDA-MB-468, and 4T1; non-TNBC MCF-7 cells; and noncancerous MCF-10A cells and PBMCs were grown to a density of 10^4 cells/ml and treated with different concentrations of NMK-T-057 (0–5 μM) for 24 h. Cell viability was evaluated by MTT assay. After treatment, MTT solution (5 mg/ml) was added to each well, and the formation of the formazan complex was measured at 595 nm using a SpectraMax 340 microplate reader (Molecular Devices). Cell viability (%) was determined using the following formula: (Absorbance of treated cells – Absorbance of medium only)/(Absorbance of untreated cells – Absorbance of medium only) \times 100. Untreated cells present in the medium were considered to be 100% viable (74).

Colony forming assay

To determine the colony-forming ability, MDA-MB-231 and MCF-7 cells were trypsinized, and single-cell suspensions were prepared. The colony forming assay was initiated by seeding the cells from single-cell suspension at a density of 10^3 cells/ml. Colony formation was monitored for 5 days in the absence and presence of NMK-T-057 (0–5 μM). Viable colonies were then stained with crystal violet, and images were taken.

Determination of apoptosis by annexin V/propidium iodide double staining

BC cells such as MDA-MB-231, MDA-MB-468, and MCF-7 cells were grown to a density of 10^4 cells/ml and then treated with different concentrations of NMK-T-057 (0–10 μM) for 24 h. Apoptosis was determined by the annexin V-FITC/PI double staining method using flow cytometry. After treatment, cells were washed twice with $1 \times$ PBS, incubated with annexin V-FITC in binding buffer, and then counterstained with PI. Results were obtained on a FACSCalibur flow cytometer (BD Biosciences) using Cell Quest software (BD Biosciences).

Determination of migration by Boyden chamber assay

Migratory properties of the breast cancer cells were determined by Boyden chamber assay using track-etched poly(ethylene terephthalate) membranes (HiMedia). BC cells such as MDA-MB-231, MDA-MB-468, and MCF-7 cells were grown to a density of 10^5 cells/ml and then treated with different concentrations of NMK-T-057 (0–10 μM) for 24 h. After treatment, cells were trypsinized and seeded in the upper chamber of the Boyden chamber at a density of 10^3 cells/ml. The whole system was incubated for 24 h at 37 °C in a humidified atmosphere with 5% CO₂. After incubation, the cells of the upper side of the membranes, which had not migrated, were removed by gently wiping with a cotton swab, and the cells that had migrated to the lower surface of the membranes were stained with crystal violet. The resultant crystal violet complex was then dissolved in 10% acetic acid, and the absorbance was measured at 600 nm

using a microplate reader (SpectraMax 340) to determine the extent of migration.

Immunofluorescence microscopy

Cultured MDA-MB-231 cells were grown on glass coverslips and then treated with NMK-T-057 (0–5 μM) for 24 h. Treated cells were washed with PBS and fixed with 2% formaldehyde for 30 min upon incubation at room temperature. Cells were then permeabilized by incubation with sodium citrate buffer (0.1% sodium citrate and 0.1% Triton X-100) for 15 min, and nonspecific binding was blocked with 5% BSA. The F-actin network was stained using the actin-specific dye phalloidin-FITC (1:100 dilution), and images were obtained with an Olympus LSM IX81 confocal microscope.

Mammosphere assay

The ability of MDA-MB-231 cells to form spheres in the presence and absence of NMK-T-057 was monitored by mammosphere assay following the protocol published previously (43). Cultured MDA-MB-231 cells were grown to a density of 1×10^5 cells/ml and then treated with different concentrations of NMK-T-057 (0–5 μM) for 24 h. After treatment, cells were seeded in 6-well ultralow-attachment plates at a density of 1×10^4 cells/ml in each well containing DMEM/F-12 medium supplemented with recombinant epidermal growth factor (20 ng/ml), bovine insulin (5 $\mu\text{g}/\text{ml}$), B27 supplement, and antibiotic-antimycotic mixture. The culture of the primary mammospheres was continued up to 7 days, and images of the spheres from each set were taken to quantify the number of spheres formed. For serial passaging, mammospheres were enzymatically dissociated into single cells and reseeded in low-attachment plates to monitor the formation of secondary mammospheres.

Determination of CD44^{high}/CD24^{low} population by flow cytometry

Cultured MDA-MB-231 cells were grown to a density of 10^5 cells/ml and then treated with different concentrations of NMK-T-057 (0–5 μM) for 24 h. Next, the status of the CD44^{high}/CD24^{low} population in control and NMK-treated cells was determined by flow cytometry following a published/standard protocol (43). After treatment, cells were resuspended in buffer and incubated with PE-conjugated CD44 and FITC-conjugated CD24. The CD44^{high}/CD24^{low} population was determined using flow cytometry (BD FACSAria[™] III, BD Biosciences), and the results were analyzed using BD FACSDiva v6.1.3/v.7 software.

Detection of ALDH⁺ population by flow cytometry

Enhanced expression and activity of ALDH1 enzyme is known to be a hallmark of cancer stem cells in several malignancies, including breast cancer (42, 75). The stem cell-enriched ALDH⁺ population can be determined by FACS using the ALDEFLUOR[™] assay kit (43). Cultured MDA-MB-231 cells were grown to a density of 1×10^5 cells/ml and then treated with different concentrations of NMK-T-057 (0–5 μM) for 24 h. After treatment, cells were suspended in ALDEFLUOR assay buffer containing ALDH substrate (Bodipy-aminoacetal-

dehyde) and processed further following the manufacturer's protocol. ALDH1-expressing cells (ALDH1^{high}) showing bright fluorescence were quantified using the green fluorescence channel (520–540 nm) of FACSAria III.

siRNA/plasmid transfection

Cultured MDA-MB-231 cells were transfected with 100 nM control scrambled siRNA or si-Notch-1 using Lipofectamine 2000 according to the manufacturer's instructions and incubated in Opti-MEM for 24 h. After 24 h, Opti-MEM was replaced with normal growth medium, and cells were harvested after a further 48 h of incubation.

The activated NOTCH1 (pEGFP-NICD) and empty vector constructs were obtained as a generous gifts from Dr. Amit Dutt (Tata Memorial Centre Advanced Centre for Treatment, Research and Education in Cancer (ACTREC), Mumbai, India). Cultured MCF-7 cells were transfected with each of the plasmids (500 μ g/ml) using Lipofectamine 2000 according to the manufacturer's instructions.

In vitro γ -secretase assay

γ -Secretase activity in MDA-MB-231 and MDA-MB-468 cells was measured using the fluorogenic substrate NMA-Gly-Cys-**Gly-Val-Leu**-Leu-Lys(dnp)-Arg-Arg-NH₂ trifluoroacetate (Sigma-Aldrich) following the manufacturer's protocol. To perform the γ -secretase assay, membrane fractions were first prepared from untreated, NMK-treated (0–10 μ M), and DAPT-treated (0–10 μ M) MDA-MB-231 and MDA-MB-468 cells using a Qproteome Cell Compartment kit. Briefly, cell suspensions from NMK/DAPT-treated and untreated cells (~10⁶ cells/ml) were prepared and centrifuged at 500 \times g for 10 min at 4 °C. The supernatant was discarded carefully, and the pellet was suspended in 1 ml of ice-cold Extraction Buffer CE1 for 10 min at 4 °C under shaking conditions. The suspension was then centrifuged at 1000 \times g for 10 min at 4 °C. The supernatant containing the cytosolic proteins was discarded, and the pellet was suspended in 1 ml of ice-cold Extraction Buffer CE2 for 10 min at 4 °C under shaking conditions. The suspension was then centrifuged at 6000 \times g for 10 min at 4 °C, and the supernatant containing the membrane proteins was collected. Total protein present in the membrane fraction was measured using the Bradford protein estimation kit. Approximately 100 μ g of membrane proteins from each sample was incubated with 10 μ M fluorogenic substrate for 5 h at 37 °C, and fluorescence was monitored at 335-nm excitation and 440-nm emission.

In silico docking studies

To identify the putative binding site of the novel compound and DAPT on γ -secretase tetramer, molecular docking was performed using UCSF Chimera 1.11 and AutodockTools 1.5.6, the most widely used docking program (76). MarvinSketch 16.3.28 was used to draw and generate three-dimensional structures of ligands. The crystalline structure of γ -secretase (Protein Data Bank (PDB) code 5a63) was used as the template for the docking studies. Blind docking was performed using Autodock Vina (UCSF Chimera 1.11), considering a grid box covering the whole protein molecule. The best favorable site was further studied for docking using Autodock 4.1 (Autodock-

Tools 1.5.6). Grid boxes of 60 \times 60 \times 60 grid point with grid spacing 0.375 Å were constructed around the center coordinate of the active sites. The Lamarckian genetic algorithm was employed with the default parameters; g_eval was set to 2,500,000 (medium). All other parameters were kept at default values. Discovery Studio Client 2016 was used for molecular graphics and analysis of interactions.

Detection of autophagic vacuoles by the fluorescent dye monodansylcadaverine (MDC)

Cultured MDA-MB-231 cells were grown to a density of 10⁴ cells/ml and then treated with different concentrations of NMK-T-057 (0–5 μ M) and DAPT (10 μ M) for 24 h. Formation of autophagic vacuoles was monitored by confocal microscopy as well as FACS using the fluorescent dye MDC. For flow cytometry, treated and untreated cells were stained with MDC by incubating cells with 0.05 mM MDC at 37 °C for 30 min. After incubation, cells were washed three times with PBS, and the MDC-positive population was quantified using a FACSCalibur flow cytometer. The data were then analyzed using Cell Quest software.

For confocal microscopy, cultured MDA-MB-231 cells were grown on sterile glass coverslips and subjected to treatment with the above-mentioned compounds. After 24 h of treatment, old medium was replaced with new medium containing 0.05 mM MDC. Control and NMK/DAPT-treated cells were incubated with medium containing 0.05 mM MDC for 30 min at 37 °C. After incubation, each set was washed thrice with 1 \times PBS and incubated with propidium iodide (1 μ g/ml) for 5 min at room temperature to stain the nucleus. The images were captured by an Olympus LSM IX81 confocal microscope. To monitor the effect of autophagy inhibitor, prior to NMK/DAPT treatment cells were pretreated with 500 μ M 3-MA for 1 h.

Western blot analysis

Western blot analysis was performed to determine the expression levels of the EMT-related proteins such as vimentin, N-cadherin, E-cadherin, keratin-19, and TWIST; Notch-targeting proteins such as Notch-1 (NICD), Hes-1, PTEN, pAkt, and Akt; and autophagy markers such as LC3 and Beclin in control and NMK-treated MDA-MB-231 cells. After treatment, cell lysates were prepared by adding lysis buffer containing 50 mM Tris-HCl, pH 8.0, 0.1% SDS, 150 mM NaCl, 1% Nonidet P-40, and a protease inhibitor mixture including 1 μ g/ml aprotinin, 1 μ g of leupeptin, and 1.0 mM phenylmethylsulfonyl fluoride. Equal amounts of protein were loaded for 7.5–10% SDS-PAGE and transferred onto a nitrocellulose membrane. Membranes were incubated with specific primary antibodies overnight followed by secondary antibodies. Primary and secondary antibody dilutions were made according to the manufacturer's protocols.

Tumor formation in female BALB/c mice by 4T1 xenograft

Cultured 4T1 cells (2 \times 10⁵) were suspended in 0.1 ml of PBS and injected subcutaneously into the mammary fat pad of each mouse for the development of palpable tumor (>50 mm³). After tumor development, mice were divided into control and treatment groups (n = 6). In the treatment group, mice were

NMK-T-057 inhibits γ -secretase-mediated Notch activation

injected intraperitoneally (alternate days) with different doses of NMK-T-057 (10, 25, and 50 mg/kg-BW) once for 15 days. After 15 days of treatment, mice were euthanized, and dissected tumors were collected for further investigations. Tumor volume was calculated by the following formula: $0.5 \times w^2 \times l$ where w is width and l is length (77).

Immunohistochemistry

All immunohistochemistry experiments were performed using a Histostain-Plus IHC kit (Life Technologies) following the protocol published previously (77). Briefly, after microwave treatment of deparaffinized sections in citrate buffer and endogenous peroxide blocking, the sections were incubated in specific antibody solution overnight at 4 °C in a moist chamber. The immunoreactivity was detected by 3,3'-diaminobenzidine, and the sections were counterstained with hematoxylin.

Statistical analysis

All data are presented as the mean \pm S.E. of n independent measurements as indicated in the corresponding figure legends. Statistical comparisons between treated and untreated control groups were calculated by Student's t tests using GraphPad Prism 6, and multiple groups were compared by analysis of variance test using Newman-Keuls post-analysis. A value of $p < 0.05$ was considered significant.

Author contributions—A. D. and G. C. conceptualization; A. D., S. C., M. P., S. K. B., and P. K. data curation; A. D. and U. C. formal analysis; A. D. and G. C. funding acquisition; A. D., S. P., P. M., D. G. D., A. G., B. B., and D. K. investigation; A. D., M. K. N., S. P., P. M., S. G., M. P., S. K. B., and D. K. methodology; A. D. and S. P. writing-original draft; D. G. D. software; M. P. resources; M. P., U. C., D. K., and G. C. writing-review and editing; G. C. supervision; G. C. project administration.

Acknowledgment—We acknowledge Dr. Amit Dutt (Tata Memorial Centre Advanced Centre for Treatment, Research and Education in Cancer (ACTREC), Mumbai, India) for providing the activated NOTCH1 (pEGFP-NICD) and empty vector constructs.

References

1. Ferlay, J., Soerjomataram, I., Dikshit, R., Eser, S., Mathers, C., Rebelo, M., Parkin, D. M., Forman, D., and Bray, F. (2015) Cancer incidence and mortality worldwide: sources, methods and major patterns in GLOBOCAN 2012. *Int. J. Cancer*. **136**, E359–E386 [CrossRef Medline](#)
2. Torre, L. A., Siegel, R. L., Ward, E. M., and Jemal, A. (2016) Global cancer incidence and mortality rates and trends—an update. *Cancer Epidemiol. Biomarkers Prev.* **25**, 16–27 [CrossRef Medline](#)
3. Ghoncheh, M., Momenimovahed, Z., and Salehiniya, H. (2016) Epidemiology, incidence and mortality of breast cancer in Asia. *Asian Pac. J. Cancer Prev.* **17**, 47–52 [CrossRef Medline](#)
4. Gupta, S. (2016) Breast cancer: Indian experience, data, and evidence. *South Asian J. Cancer* **5**, 85–86 [CrossRef Medline](#)
5. Sørlie, T., Perou, C. M., Tibshirani, R., Aas, T., Geisler, S., Johnsen, H., Hastie, T., Eisen, M. B., van de Rijn, M., Jeffrey, S. S., Thorsen, T., Quist, H., Matese, J. C., Brown, P. O., Botstein, D., et al. (2001) Gene expression patterns of breast carcinomas distinguish tumor subclasses with clinical implications. *Proc. Natl. Acad. Sci. U.S.A.* **98**, 10869–10874 [CrossRef Medline](#)
6. Rakha, E. A., Tan, D. S., Foulkes, W. D., Ellis, I. O., Tutt, A., Nielsen, T. O., and Reis-Filho, J. S. (2007) Are triple-negative tumours and basal-like breast cancer synonymous? *Breast Cancer Res.* **9**, 404 [CrossRef Medline](#)
7. Rodríguez-Pinilla, S. M., Sarrió, D., Honrado, E., Hardisson, D., Calero, F., Benitez, J., and Palacios, J. (2006) Prognostic significance of basal-like phenotype and fascin expression in node-negative invasive breast carcinomas. *Clin. Cancer Res.* **12**, 1533–1539 [CrossRef Medline](#)
8. Haque, I., De, A., Majumder, M., Mehta, S., McGregor, D., Banerjee, S. K., Van Veldhuizen, P., and Banerjee, S. (2012) The matricellular protein CCN1/Cyr61 is a critical regulator of Sonic Hedgehog in pancreatic carcinogenesis. *J. Biol. Chem.* **287**, 38569–38579 [CrossRef Medline](#)
9. Koch, U., and Radtke, F. (2007) Notch and cancer: a double-edged sword. *Cell. Mol. Life Sci.* **64**, 2746–2762 [CrossRef Medline](#)
10. Sriuranpong, V., Borges, M. W., Ravi, R. K., Arnold, D. R., Nelkin, B. D., Baylin, S. B., and Ball, D. W. (2001) Notch signaling induces cell cycle arrest in small cell lung cancer cells. *Cancer Res.* **61**, 3200–3205 [Medline](#)
11. Wang, Z., Li, Y., Banerjee, S., and Sarkar, F. H. (2008) Exploitation of the Notch signaling pathway as a novel target for cancer therapy. *Anticancer Res.* **28**, 3621–3630 [Medline](#)
12. Cho, S., Lu, M., He, X., Ee, P. L., Bhat, U., Schneider, E., Miele, L., and Beck, W. T. (2011) Notch1 regulates the expression of the multidrug resistance gene ABCB1/MRP1 in cultured cancer cells. *Proc. Natl. Acad. Sci. U.S.A.* **108**, 20778–20783 [CrossRef Medline](#)
13. Reedijk, M., Odorcic, S., Chang, L., Zhang, H., Miller, N., McCready, D. R., Lockwood, G., and Egan, S. E. (2005) High-level coexpression of JAG1 and NOTCH1 is observed in human breast cancer and is associated with poor overall survival. *Cancer Res.* **65**, 8530–8537 [CrossRef Medline](#)
14. Stylianou, S., Clarke, R. B., and Brennan, K. (2006) Aberrant activation of notch signaling in human breast cancer. *Cancer Res.* **66**, 1517–1525 [CrossRef Medline](#)
15. Wang, Z., Li, Y., Ahmad, A., Azmi, A. S., Banerjee, S., Kong, D., and Sarkar, F. H. (2010) Targeting Notch signaling pathway to overcome drug resistance for cancer therapy. *Biochim. Biophys. Acta* **1806**, 258–267 [CrossRef Medline](#)
16. Bolós, V., Mira, E., Martínez-Poveda, B., Luxán, G., Cañamero, M., Martínez-A, C., Mañes, S., and de la Pompa, J. L. (2013) Notch activation stimulates migration of breast cancer cells and promotes tumor growth. *Breast Cancer Res.* **15**, R54 [CrossRef Medline](#)
17. Guo, S., Liu, M., and Gonzalez-Perez, R. R. (2011) Role of Notch and its oncogenic signaling crosstalk in breast cancer. *Biochim. Biophys. Acta* **1815**, 197–213 [CrossRef Medline](#)
18. Boyle, S. T., Gieniec, K. A., Gregor, C. E., Faulkner, J. W., McColl, S. R., and Kochetkova, M. (2017) Interplay between CCR7 and Notch1 axes promotes stemness in MMTV-PyMT mammary cancer cells. *Mol. Cancer* **16**, 19 [CrossRef Medline](#)
19. Pal, D., Kolluru, V., Chandrasekaran, B., Baby, B. V., Aman, M., Suman, S., Sirimulla, S., Sanders, M. A., Alatas, H., Ankem, M. K., and Damodaran, C. (2017) Targeting aberrant expression of Notch-1 in ALDH+ cancer stem cells in breast cancer. *Mol. Carcinog.* **56**, 1127–1136 [CrossRef Medline](#)
20. Zhong, Y., Shen, S., Zhou, Y., Mao, F., Lin, Y., Guan, J., Xu, Y., Zhang, S., Liu, X., and Sun, Q. (2016) NOTCH1 is a poor prognostic factor for breast cancer and is associated with breast cancer stem cells. *Onco Targets Ther.* **9**, 6865–6871 [CrossRef Medline](#)
21. Al-Hussaini, H., Subramanyam, D., Reedijk, M., and Sridhar, S. S. (2011) Notch signaling pathway as a therapeutic target in breast cancer. *Mol. Cancer Ther.* **10**, 9–15 [CrossRef Medline](#)
22. Grudzien, P., Lo, S., Albain, K. S., Robinson, P., Rajan, P., Strack, P. R., Golde, T. E., Miele, L., and Foreman, K. E. (2010) Inhibition of Notch signaling reduces the stem-like population of breast cancer cells and prevents mammosphere formation. *Anticancer Res.* **30**, 3853–3867 [Medline](#)
23. Borggreffe, T., and Oswald, F. (2009) The Notch signaling pathway: transcriptional regulation at Notch target genes. *Cell. Mol. Life Sci.* **66**, 1631–1646 [CrossRef Medline](#)
24. Zhang, Y. W., Luo, W. J., Wang, H., Lin, P., Vetrivel, K. S., Liao, F., Li, F., Wong, P. C., Farquhar, M. G., Thinakaran, G., and Xu, H. (2005) Nicastrin is critical for stability and trafficking but not association of other presenilin/ γ -secretase components. *J. Biol. Chem.* **280**, 17020–17026 [CrossRef Medline](#)

25. Palomero, T., Dominguez, M., and Ferrando, A. A. (2008) The role of the PTEN/AKT pathway in NOTCH1-induced leukemia. *Cell Cycle* **7**, 965–970 [CrossRef Medline](#)
26. Schott, A. F., Landis, M. D., Dontu, G., Griffith, K. A., Layman, R. M., Krop, I., Paskett, L. A., Wong, H., Dobrolecki, L. E., Lewis, M. T., Froehlich, A. M., Parani, J., Hayes, D. F., Wicha, M. S., and Chang, J. C. (2013) Preclinical and clinical studies of gamma secretase inhibitors with docetaxel on human breast tumors. *Clin. Cancer Res.* **19**, 1512–1524 [CrossRef Medline](#)
27. Yuan, X., Wu, H., Xu, H., Xiong, H., Chu, Q., Yu, S., Wu, G. S., and Wu, K. (2015) Notch signaling: an emerging therapeutic target for cancer treatment. *Cancer Lett.* **369**, 20–27 [CrossRef Medline](#)
28. de Sá Alves, F. R., Barreiro, E. J., and Fraga, C. A. (2009) From nature to drug discovery: the indole scaffold as a 'privileged structure'. *Mini Rev. Med. Chem.* **9**, 782–793 [CrossRef Medline](#)
29. Kumar, D., Narayanam, M. K., Chang, K. H., and Shah, K. (2011) Synthesis of novel indolyl-1,2,4-triazoles as potent and selective anticancer agents. *Chem. Biol. Drug Des.* **77**, 182–188 [CrossRef Medline](#)
30. Sztanke, K., Pasternak, K., Rzymowska, J., Sztanke, M., and Kandefer-Szerszeń, M. (2008) Synthesis, structure elucidation and identification of antitumoural properties of novel fused 1,2,4-triazine aryl derivatives. *Eur. J. Med. Chem.* **43**, 1085–1094 [CrossRef Medline](#)
31. Sztanke, K., Tuzimski, T., Rzymowska, J., Pasternak, K., and Kandefer-Szerszeń, M. (2008) Synthesis, determination of the lipophilicity, anticancer and antimicrobial properties of some fused 1,2,4-triazole derivatives. *Eur. J. Med. Chem.* **43**, 404–419 [CrossRef Medline](#)
32. Genc, M., Karagoz Genc, Z., Tekin, S., Sandal, S., Sirajuddin, M., Hadda Taibi, B., and Sekerci, M. (2016) Design, synthesis, *in vitro* antiproliferative activity, binding modeling of 1,2,4-triazoles as new anti-breast cancer agents. *Acta Chim. Slov.* **63**, 726–737 [Medline](#)
33. Mioc, M., Soica, C., Bercean, V., Avram, S., Balan-Porcarasu, M., Coricovac, D., Ghiulai, R., Muntean, D., Andrica, F., Dehelean, C., Spandidos, D. A., Tsatsakis, A. M., and Kurunczi, L. (2017) Design, synthesis and pharmacotoxicological assessment of 5-mercapto-1,2,4-triazole derivatives with antibacterial and antiproliferative activity. *Int. J. Oncol.* **50**, 1175–1183 [CrossRef Medline](#)
34. Espinoza, I., and Miele, L. (2013) Deadly crosstalk: Notch signaling at the intersection of EMT and cancer stem cells. *Cancer Lett.* **341**, 41–45 [CrossRef Medline](#)
35. Suman, S., Das, T. P., and Damodaran, C. (2013) Silencing NOTCH signaling causes growth arrest in both breast cancer stem cells and breast cancer cells. *Br. J. Cancer* **109**, 2587–2596 [CrossRef Medline](#)
36. Ray, A., Vasudevan, S., and Sengupta, S. (2015) 6-Shogaol inhibits breast cancer cells and stem cell-like spheroids by modulation of Notch signaling pathway and induction of autophagic cell death. *PLoS One* **10**, e0137614 [CrossRef Medline](#)
37. Wang, Y., Wang, H., Ge, H., and Yang, Z. (2018) AG-1031 induced autophagic cell death and apoptosis in C6 glioma cells associated with Notch-1 signaling pathway. *J. Cell. Biochem.* **119**, 5893–5903 [CrossRef Medline](#)
38. Christofori, G. (2006) New signals from the invasive front. *Nature* **441**, 444–450 [CrossRef Medline](#)
39. Haynes, J., Srivastava, J., Madson, N., Wittmann, T., and Barber, D. L. (2011) Dynamic actin remodeling during epithelial-mesenchymal transition depends on increased moesin expression. *Mol. Biol. Cell* **22**, 4750–4764 [CrossRef Medline](#)
40. Jin, J., Krishnamachary, B., Mironchik, Y., Kobayashi, H., and Bhujwala, Z. M. (2016) Phototheranostics of CD44-positive cell populations in triple negative breast cancer. *Sci. Rep.* **6**, 27871 [CrossRef Medline](#)
41. Sheridan, C., Kishimoto, H., Fuchs, R. K., Mehrotra, S., Bhat-Nakshatri, P., Turner, C. H., Goulet, R., Jr., Badve, S., and Nakshatri, H. (2006) CD44+/CD24- breast cancer cells exhibit enhanced invasive properties: an early step necessary for metastasis. *Breast Cancer Res.* **8**, R59 [CrossRef Medline](#)
42. Lohberger, B., Rinner, B., Stüendl, N., Absenger, M., Liegl-Atzwanger, B., Walzer, S. M., Windhager, R., and Leithner, A. (2012) Aldehyde dehydrogenase 1, a potential marker for cancer stem cells in human sarcoma. *PLoS One* **7**, e43664 [CrossRef Medline](#)
43. Mukherjee, P., Gupta, A., Chattopadhyay, D., and Chatterji, U. (2017) Modulation of SOX2 expression delineates an end-point for paclitaxel-effectiveness in breast cancer stem cells. *Sci. Rep.* **7**, 9170 [CrossRef Medline](#)
44. Dontu, G., Abdallah, W. M., Foley, J. M., Jackson, K. W., Clarke, M. F., Kawamura, M. J., and Wicha, M. S. (2003) *In vitro* propagation and transcriptional profiling of human mammary stem/progenitor cells. *Genes Dev.* **17**, 1253–1270 [CrossRef Medline](#)
45. Gupta, P. B., Onder, T. T., Jiang, G., Tao, K., Kuperwasser, C., Weinberg, R. A., and Lander, E. S. (2009) Identification of selective inhibitors of cancer stem cells by high-throughput screening. *Cell* **138**, 645–659 [CrossRef Medline](#)
46. Mani, S. A., Guo, W., Liao, M. J., Eaton, E. N., Ayyanan, A., Zhou, A. Y., Brooks, M., Reinhard, F., Zhang, C. C., Shipitsin, M., Campbell, L. L., Polyak, K., Briskin, C., Yang, J., and Weinberg, R. A. (2008) The epithelial-mesenchymal transition generates cells with properties of stem cells. *Cell* **133**, 704–715 [CrossRef Medline](#)
47. Grimshaw, M. J., Cooper, L., Papazisis, K., Coleman, J. A., Bohnenkamp, H. R., Chiapero-Stanke, L., Taylor-Papadimitriou, J., and Burchell, J. M. (2008) Mammosphere culture of metastatic breast cancer cells enriches for tumorigenic breast cancer cells. *Breast Cancer Res.* **10**, R52 [CrossRef Medline](#)
48. Ponti, D., Costa, A., Zaffaroni, N., Pratesi, G., Petrangolini, G., Coradini, D., Pilotti, S., Pierotti, M. A., and Daidone, M. G. (2005) Isolation and *in vitro* propagation of tumorigenic breast cancer cells with stem/progenitor cell properties. *Cancer Res.* **65**, 5506–5511 [CrossRef Medline](#)
49. Al-Hajj, M., Wicha, M. S., Benito-Hernandez, A., Morrison, S. J., and Clarke, M. F. (2003) Prospective identification of tumorigenic breast cancer cells. *Proc. Natl. Acad. Sci. U.S.A.* **100**, 3983–3988 [CrossRef Medline](#)
50. Balko, J. M., Cook, R. S., Vaught, D. B., Kuba, M. G., Miller, T. W., Bhola, N. E., Sanders, M. E., Granja-Ingram, N. M., Smith, J. J., Meszoely, I. M., Salter, J., Dowsett, M., Stemke-Hale, K., González-Angulo, A. M., Mills, G. B., *et al.* (2012) Profiling of residual breast cancers after neoadjuvant chemotherapy identifies DUSP4 deficiency as a mechanism of drug resistance. *Nat. Med.* **18**, 1052–1059 [CrossRef Medline](#)
51. Creighton, C. J., Li, X., Landis, M., Dixon, J. M., Neumeister, V. M., Sjolund, A., Rimm, D. L., Wong, H., Rodriguez, A., Herschkowitz, J. I., Fan, C., Zhang, X., He, X., Pavlick, A., Gutierrez, M. C., *et al.* (2009) Residual breast cancers after conventional therapy display mesenchymal as well as tumor-initiating features. *Proc. Natl. Acad. Sci. U.S.A.* **106**, 13820–13825 [CrossRef Medline](#)
52. Efferson, C. L., Winkelmann, C. T., Ware, C., Sullivan, T., Giampaoli, S., Tammam, J., Patel, S., Mesiti, G., Reilly, J. F., Gibson, R. E., Buser, C., Yeatman, T., Coppola, D., Winter, C., Clark, E. A., *et al.* (2010) Downregulation of Notch pathway by a gamma-secretase inhibitor attenuates AKT/mammalian target of rapamycin signaling and glucose uptake in an ERBB2 transgenic breast cancer model. *Cancer Res.* **70**, 2476–2484 [CrossRef Medline](#)
53. Meurette, O., Stylianou, S., Rock, R., Collu, G. M., Gilmore, A. P., and Brennan, K. (2009) Notch activation induces Akt signaling via an autocrine loop to prevent apoptosis in breast epithelial cells. *Cancer Res.* **69**, 5015–5022 [CrossRef Medline](#)
54. Hage, S., Marinangeli, C., Stanga, S., Octave, J. N., Quetin-Leclercq, J., and Kienlen-Campard, P. (2014) γ -Secretase inhibitor activity of a *Pterocarpus erinaceus* extract. *Neurodegener. Dis.* **14**, 39–51 [CrossRef Medline](#)
55. Morohashi, Y., Kan, T., Tominari, Y., Fuwa, H., Okamura, Y., Watanabe, N., Sato, C., Natsugari, H., Fukuyama, T., Iwatsubo, T., and Tomita, T. (2006) C-terminal fragment of presenilin is the molecular target of a dipeptidic γ -secretase-specific inhibitor DAPT (*N*-[*N*-(3,5-difluorophenacetyl)-*L*-alanyl]-*S*-phenylglycine *t*-butyl ester). *J. Biol. Chem.* **281**, 14670–14676 [CrossRef Medline](#)
56. Ganguli, A., Das, A., Nag, D., Bhattacharya, S., and Chakrabarti, G. (2016) Potential role of autophagy in smokeless tobacco extract-induced cytotoxicity and in morin-induced protection in oral epithelial cells. *Food Chem. Toxicol.* **90**, 160–170 [CrossRef Medline](#)
57. Chaabane, W., User, S. D., El-Gazzah, M., Jaksik, R., Sajjadi, E., Rzeszowska-Wolny, J., and Los, M. J. (2013) Autophagy, apoptosis, mitop-

NMK-T-057 inhibits γ -secretase-mediated Notch activation

- tosis and necrosis: interdependence between those pathways and effects on cancer. *Arch. Immunol. Ther. Exp.* **61**, 43–58 [CrossRef Medline](#)
58. Artavanis-Tsakonas, S., Rand, M. D., and Lake, R. J. (1999) Notch signaling: cell fate control and signal integration in development. *Science* **284**, 770–776 [CrossRef Medline](#)
59. Azzam, D. J., Zhao, D., Sun, J., Minn, A. J., Ranganathan, P., Drews-Elger, K., Han, X., Picon-Ruiz, M., Gilbert, C. A., Wander, S. A., Capobianco, A. J., El-Ashry, D., and Slingerland, J. M. (2013) Triple negative breast cancer initiating cell subsets differ in functional and molecular characteristics and in gamma-secretase inhibitor drug responses. *EMBO Mol. Med.* **5**, 1502–1522 [CrossRef Medline](#)
60. Wu, X., Fleming, A., Ricketts, T., Pavel, M., Virgin, H., Menzies, F. M., and Rubinsztein, D. C. (2016) Autophagy regulates Notch degradation and modulates stem cell development and neurogenesis. *Nat. Commun.* **7**, 10533 [CrossRef Medline](#)
61. Bhoopathi, P., Chetty, C., Gujrati, M., Dinh, D. H., Rao, J. S., and Lakka, S. (2010) Cathepsin B facilitates autophagy-mediated apoptosis in SPARC overexpressed primitive neuroectodermal tumor cells. *Cell Death Differ.* **17**, 1529–1539 [CrossRef Medline](#)
62. Liu, W., Wang, X., Sun, J., Yang, Y., Li, W., and Song, J. (2017) Parthenolide suppresses pancreatic cell growth by autophagy-mediated apoptosis. *Onco Targets Ther.* **10**, 453–461 [CrossRef Medline](#)
63. Ranjan, A., and Srivastava, S. K. (2016) Penfluridol suppresses pancreatic tumor growth by autophagy-mediated apoptosis. *Sci. Rep.* **6**, 26165 [CrossRef Medline](#)
64. Chen, Q., Kang, J., and Fu, C. (2018) The independence of and associations among apoptosis, autophagy, and necrosis. *Signal Transduct. Target Ther.* **3**, 18 [CrossRef Medline](#)
65. Liu, Y., and Levine, B. (2015) Autosis and autophagic cell death: the dark side of autophagy. *Cell Death Differ.* **22**, 367–376 [CrossRef Medline](#)
66. Su, F., Zhu, S., Ruan, J., Muftuoglu, Y., Zhang, L., and Yuan, Q. (2016) Combination therapy of RY10–4 with the γ -secretase inhibitor DAPT shows promise in treating HER2-amplified breast cancer. *Oncotarget* **7**, 4142–4154 [CrossRef Medline](#)
67. Tamagnone, L., Zacchigna, S., and Rehman, M. (2018) Taming the Notch transcriptional regulator for cancer therapy. *Molecules* **23**, E431 [CrossRef Medline](#)
68. Cui, J., Wang, Y., Dong, B., Qin, L., Wang, C., Zhou, P., Wang, X., Xu, H., Xue, W., Fang, Y. X., and Gao, W. Q. (2018) Pharmacological inhibition of the Notch pathway enhances the efficacy of androgen deprivation therapy for prostate cancer. *Int. J. Cancer* **143**, 645–656 [CrossRef Medline](#)
69. Dai, G., Deng, S., Guo, W., Yu, L., Yang, J., Zhou, S., and Gao, T. (2019) Notch pathway inhibition using DAPT, a γ -secretase inhibitor (GSI), enhances the antitumor effect of cisplatin in resistant osteosarcoma. *Mol. Carcinog.* **58**, 3–18 [CrossRef Medline](#)
70. Mao, L., Zhao, Z. L., Yu, G. T., Wu, L., Deng, W. W., Li, Y. C., Liu, J. F., Bu, L. L., Liu, B., Kulkarni, A. B., Zhang, W. F., Zhang, L., and Sun, Z. J. (2018) γ -Secretase inhibitor reduces immunosuppressive cells and enhances tumour immunity in head and neck squamous cell carcinoma. *Int. J. Cancer* **142**, 999–1009 [CrossRef Medline](#)
71. McGowan, P. M., Simeone, C., Ribot, E. J., Foster, P. J., Palmieri, D., Steeg, P. S., Allan, A. L., and Chambers, A. F. (2011) Notch1 inhibition alters the CD44hi/CD24lo population and reduces the formation of brain metastases from breast cancer. *Mol. Cancer Res.* **9**, 834–844 [CrossRef Medline](#)
72. Chatterjee, A., and Chatterji, U. (2017) All-trans retinoic acid ameliorates arsenic-induced oxidative stress and apoptosis in the rat uterus by modulating MAPK signaling proteins. *J. Cell. Biochem.* **118**, 3796–3809 [CrossRef Medline](#)
73. Strickley, R. G. (2004) Solubilizing excipients in oral and injectable formulations. *Pharm. Res.* **21**, 201–230 [CrossRef Medline](#)
74. Gupta, S., Prasad, G. V., and Mukhopadhyaya, A. (2015) *Vibrio cholerae* porin OmpU induces caspase-independent programmed cell death upon translocation to the host cell mitochondria. *J. Biol. Chem.* **290**, 31051–31068 [CrossRef Medline](#)
75. Tomita, H., Tanaka, K., Tanaka, T., and Hara, A. (2016) Aldehyde dehydrogenase 1A1 in stem cells and cancer. *Oncotarget* **7**, 11018–11032 [CrossRef Medline](#)
76. Morris, G. M., Huey, R., Lindstrom, W., Sanner, M. F., Belew, R. K., Goodsell, D. S., and Olson, A. J. (2009) AutoDock4 and AutoDockTools4: automated docking with selective receptor flexibility. *J. Comput. Chem.* **30**, 2785–2791 [CrossRef Medline](#)
77. Ghosh, A., Sarkar, S., Banerjee, S., Behbod, F., Tawfik, O., McGregor, D., Graff, S., and Banerjee, S. K. (2018) MIND model for triple-negative breast cancer in syngeneic mice for quick and sequential progression analysis of lung metastasis. *PLoS One* **13**, e0198143 [CrossRef Medline](#)